JOC The Journal of Organic Chemistry

Article

pubs.acs.org/joc

# Porphyrins Fused with Unactivated Polycyclic Aromatic Hydrocarbons

Vyacheslav V. Diev,[†] Cody W. Schlenker,[†] Kenneth Hanson,[†] Qiwen Zhong,[†] Jeramy D. Zimmerman,[‡] Stephen R. Forrest,[‡] and Mark E. Thompson*[,†]

[†]Department of Chemistry, University of Southern California, Los Angeles, California 90089, United States

[‡]Department of Electrical Engineering and Computer Science, and Physics, University of Michigan, Ann Arbor, Michigan 48109, United States

Supporting Information

**ABSTRACT:** A systematic study of the preparation of porphyrins with extended conjugation by *meso*,*β*-fusion with polycyclic aromatic hydrocarbons (PAHs) is reported. The *meso*-positions of 5,15-unsubstituted porphyrins were readily functionalized with PAHs. Ring fusion using standard Scholl reaction conditions ($FeCl_3$, dichloromethane) occurs for perylene-substituted porphyrins to give a porphyrin *β*,*meso* annulated with perylene rings (0.7:1 ratio of *syn* and *anti* isomers). The naphthalene, pyrene, and coronene derivatives do not react under Scholl conditions but are fused using thermal cyclodehydrogenation at high temperatures, giving mixtures of *syn* and *anti* isomers of the *meso*,*β*-fused porphyrins. For pyrenyl-substituted porphyrins, a thermal method gives synthetically acceptable yields (>30%). Absorption spectra of the fused porphyrins undergo a progressive bathochromic shift in a series of naphthyl ($\lambda_{max}$ = 730 nm), coronenyl ($\lambda_{max}$ = 780 nm), pyrenyl ($\lambda_{max}$ = 815 nm), and perylenyl ($\lambda_{max}$ = 900 nm) annulated porphyrins. Despite being conjugated with unsubstituted fused PAHs, the *β*,*meso*-fused porphyrins are more soluble and processable than the parent nonfused precursors. Pyrenyl-fused porphyrins exhibit strong fluorescence in the near-infrared (NIR) spectral region, with a progressive improvement in luminescent efficiency (up to 13% with $\lambda_{max}$ = 829 nm) with increasing degree of fusion. Fused pyrenyl-porphyrins have been used as broadband absorption donor materials in photovoltaic cells, leading to devices that show comparatively high photovoltaic efficiencies.

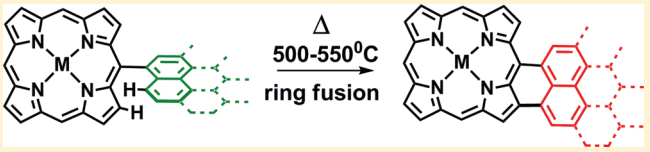


## INTRODUCTION

Porphyrins have been used in a broad range of organic electronic applications,[1−6] such as solar cells,[2,3] photodetectors,[4] light-emitting diodes,[5] and thin-film transistors,[6] because of their intense absorbance in the visible region, chemical stability and tunable optoelectronic properties.[1] Among these applications, organic photovoltaics (OPVs) have attracted a great deal of recent interest as potentially low-cost options for efficient solar energy conversion.[7] While the intense absorption bands exhibited by simple porphyrins are a benefit for use in OPVs, the comparatively narrow widths of these bands and the absence of absorption in the near-infrared (NIR) limit their utility in OPV applications. More than 50% of all solar radiation lies in the NIR and IR portions of the solar spectrum ($\lambda$ > 700 nm), so collecting light in this spectral region is critically important to improve organic solar cell performance.[2a]

Organic dyes with strong absorption and emission in the NIR spectral region are also interesting for other potential applications. The NIR region between 700−900 nm is known as the optical window for biological imaging and therapeutic applications, as this is where light has its maximum depth of penetration into tissue.[8] Large, $\pi$-conjugated macrocycles, including porphyrins, are also good candidates for two-photon dyes because of their high transition dipole moments.[9]

Extending the $\pi$-system can markedly red shift the absorption of porphyrins relative to unsubstituted derivatives.[1,10−12] One method to extend the porphyrin $\pi$-system has been to construct oligomers coupled through unsaturated bridges[11] or by *β*-fusion of *meso*-linked oligomers into so-called porphyrin "tapes".[12] While these materials lead to red-shifted absorbance (beyond 2000 nm), such oligomeric compounds typically require multistep synthesis with low overall yields.[11,12] Moreover, these oligomers show pronounced aggregation in solution and poor processability unless substituted with bulky solubilizing groups.[11,12] Very short $S_1$ excited state lifetimes for the porphyrin tapes also limits their application in a number of areas that exploit luminescence in the NIR.[12d,13] We have chosen to explore the $\pi$-extension of porphyrins by fusing polycyclic aromatic hydrocarbons (PAHs) at the *β* and *meso* positions to create materials related to molecular graphenes.[14] A schematic illustration of the direct fusion reaction studied is shown in Scheme 1, along with the PAHs used in this study. Advantages of the target porphyrin-PAH hybrids include their precisely defined structures, significant $\pi$-extension with relatively low mass and the potential for large-scale preparation.[14]

Fusion of *meso*-bound polycyclic aromatic rings has attracted significant attention recently, with both *β*,*meso* and *β*,*meso*,*β* modes for fusion reported.[15−17] Fusion in the *β*,*meso*,*β* mode,

**Received:** August 1, 2011
**Published:** November 13, 2011

   dx.doi.org/10.1021/jo201490y | J. Org. Chem. 2012, 77, 143−159

**Scheme 1**

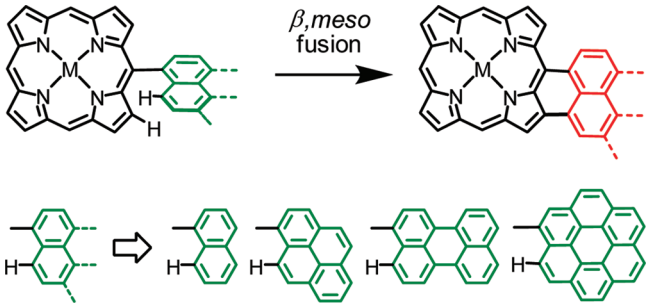


as shown by Anderson et al. in the fusion of up to four anthracene rings to a porphyrin core, leads to porphyrins with absorption shifted up to 1417 nm and with narrow line widths (full width at half-maximum (fwhm) = 284 $cm^{-1}$).[15g] Synthesis of porphyrins with fused PAH groups requires activation of the porphyrin by metalation with nickel(II) and/or activation of the singly connected aromatic rings with bulky electron donating alkoxy, aryloxy or amino groups.[15h,16f] Zinc metalated monoporphyrins with unsubstituted aromatic rings at *meso* positions have previously failed to give fused products.[15a,d] Unfortunately, metalation of porphyrins with nickel(II) causes fast deactivation of the porphyrin excited states through low-lying metal-based d-d states[18] limiting their application in a range of optoelectronic and photovoltaic applications.[15j,19] In addition, demetalation of nickel porphyrins with extended conjugation often leads to extensive decomposition,[15h,16e] or low yields of the demetalated free-base product.[15c] For these reasons we have sought synthetic approaches to *β,meso* fused porphyrin systems that require neither nickel metalation nor donor groups on the aromatic moiety to activate the system for fusion.

Development of routes to soluble graphene-like porphyrins may improve some of the material properties important in OPVs. Increasing the size of fused aromatic rings increases the relative ratio of C−C versus C−H bonds, which may impact the intermolecular interactions of the compounds in the solid state. The preference for the common herringbone packing decreases in favor of a π-stacking motif in crystal structures having a lower relative number of C−H contacts.[20] Using noncovalent π−π interactions between aromatic systems is beneficial for optoelectronic devices. Intermolecular charge transport in this case is expected to take place by a band-like, rather than hopping mechanism,[21] increasing charge carrier mobility and potentially giving improved exciton diffusion lengths in the film.[22] Depending on the spatial orientation of molecules with such a π−π overlap, significant line broadening and bathochromic shifts of the thin film absorption is also expected.[23] The presence of bulky groups is necessary for solubilizing previously reported *β,meso* fused porphyrins, but is deleterious to other materials properties such as efficient charge carrier transport[21] since the bulky group prevents π−π overlap between molecules.[15e,g,21a]

Here we present a new method for *β,meso* fusion (Scheme 1) of Zn porphyrins using direct thermal cyclodehydrogenation to effect C−H activation of *meso*-bound aromatic rings in a single step. We have investigated π-extension through *β,meso* fusion with such representative PAHs as naphthalene, pyrene, perylene and coronene *via* a preparative route that can be extended to any number of molecular graphenes. Such *β,meso* fusion of aromatic rings leads to red-shifted absorption and markedly increases line widths of the Soret and Q bands.

The precursors for *β,meso* fusion can be easily obtained by substitution with aromatic rings *via* well-developed methods (e.g., halogenation and Pd-catalyzed couplings).[11e,24] The methods described here allow for the synthesis of fused materials without added activating and solubilizing groups on the aromatic rings, or by metalation of porphyrin with nickel(II). Despite their large and unhindered π-systems, the porphyrin−PAH materials obtained have improved solubility and processability relative to their nonfused precursors. Strong NIR fluorescence is observed for the doubly fused pyrenyl derivatives, in marked contrast to poor luminescent efficiency seen in most known porphyrinoids, including porphyrin tapes.[1] Finally, we report the use of doubly fused porphyrins as NIR-absorbing donor components in organic photovoltaic cells with higher photovoltaic efficiencies compared to other reported devices that employ π-extended porphyrins.

## RESULTS AND DISCUSSION

**Synthesis.** The starting building block for our fused PAH porphyrin synthesis is a 5,15-unsubstituted porphyrin with two *meso* positions open for PAH functionalization. This building block was obtained in relatively large quantities (>30 g) using methods well-developed by Lindsey et al., starting from dipyrromethane and 3,5-di-*tert*-butyl-benzaldehyde (Scheme 2).[25] Functionalization of *meso*-H positions of the porphyrins was achieved by bromination with 1 equiv of *N*-bromosuccinimide (NBS) per *meso* position (Scheme 2).[24] Suzuki coupling reactions of the dibromoporphyrin and pinacol boronate esters of PAHs were accomplished by the use of $Pd(PPh_3)_4/Cs_2CO_3$ in toluene (Scheme 2). Yields of the *bis*-substituted derivatives **1**−**4** varied from up to 90% for *bis*-pyrenyl derivative **2** to 30−40% for *bis*-perylenyl porphyrin **3**. Preparation of pyrenyl porphyrin **2** is scalable to several grams with easy purification by crystallization. Both naphthyl (**1**) and pyrenyl (**2**) derivatives have good solubility in organic solvents (e.g., toluene, dichloromethane), whereas the solubility of the perylenyl (**3**) and coronenyl (**4**) derivatives is more limited. *Tetrakis*-pyrenyl porphyrin **5** was obtained in 30−45% yield by formation of the *bis*-pyrenyl porphyrin using commercially available pyrenecarboxaldehyde, followed by subsequent bromination of the remaining *meso* positions with NBS (2 equiv) and coupling with pyrenyl pinacol boronate ester (Scheme 3). Porphyrin **5** can also be obtained by direct condensation of pyrenecarboxaldehyde and pyrrole, albeit in lower yields than from the *bis*-pyrenyl-porphyrinic precursor.[26] The boronate ester of coronene has not previously been reported and was obtained in this study by bromination of coronene with 2−3 equiv $Br_2$ (affording an insoluble mixture of bromocoronenes), followed by borylation using HB(pin) under standard conditions and purification by column chromatography. The coronene ring has properties of extended aromatic [18]-annulenes (chemical shift in $^1H$ NMR spectra, calculated magnetic susceptibilities) due to electronic delocalization of the outer 18-membered ring.[27] Although the aromaticity of porphyrin rings is still under debate, most data suggests that porphyrin can also be described as [18]-annulene.[28] Thus, *bis*-coronenyl derivative **4** provides an unusual example of three coupled [18]-annulene units. Various metalated *bis*-pyrenyl derivatives **2-M** (M = Mg, Cu, Pb, Pd or Pt) can also be easily obtained by demetalation of **2**, followed by remetalation with the corresponding metal salts (Scheme 4).


dx.doi.org/10.1021/jo201490y | J. Org. Chem. 2012, 77, 143−159

**Scheme 2**

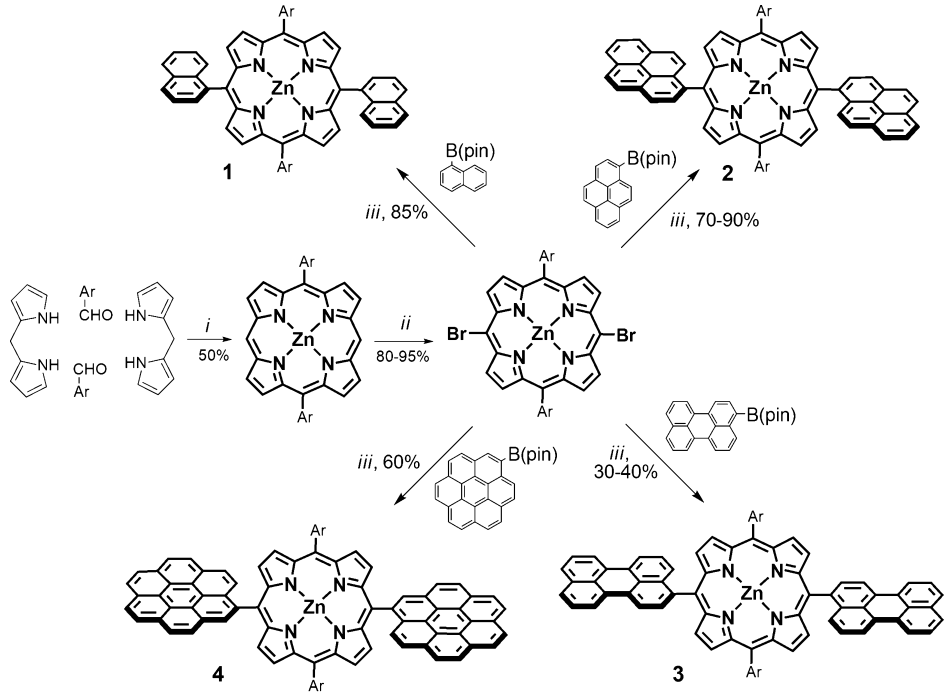


Ar = 3,5-di-*tert*-butylphenyl; *i*: a. TFA, $CH_2Cl_2$, followed by DDQ; b. $Zn(OAc)_2$, $CH_2Cl_2$, MeOH; *ii*: NBS, $CH_2Cl_2$, pyridine, -10°C; *iii*: $Pd(PPh_3)_4$, $Cs_2CO_3$, pyridine, toluene, 110°C, 10 - 20h

**Scheme 3**

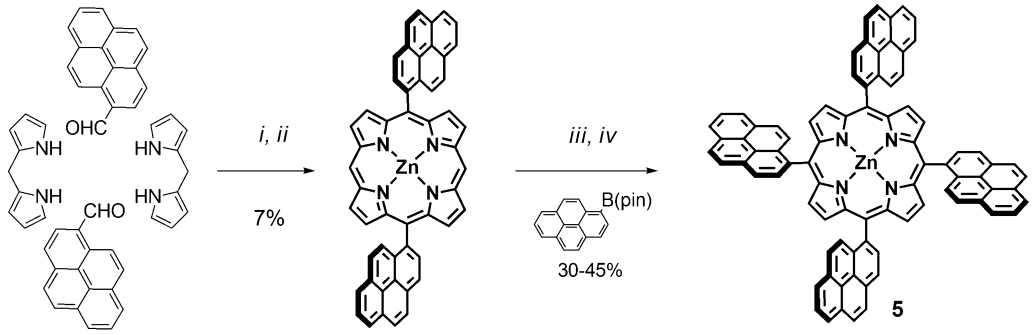


Ar = 3,5-di-*tert*-butylphenyl; *i*: TFA, $CH_2Cl_2$, r.t. 2 days, followed by DDQ; *ii*: $Zn(OAc)_2$, $CH_2Cl_2$, MeOH; *iii*: NBS, $CH_2Cl_2$, pyridine, -10°C; *iv*: $Pd(PPh_3)_4$, $Cs_2CO_3$, pyridine, toluene, 110°C, 10h

**Scheme 4**

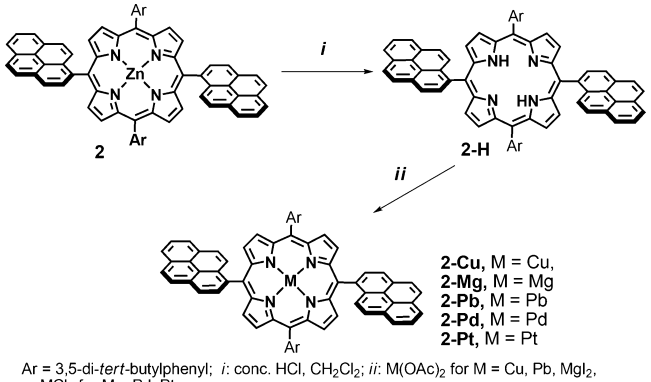


Ar = 3,5-di-*tert*-butylphenyl; *i*: conc. HCl, $CH_2Cl_2$; *ii*: $M(OAc)_2$ for M = Cu, Pb, $MgI_2$, or $MCl_2$ for M = Pd, Pt

The key step in the synthesis of fused porphyrins is a C−C fusion reaction of a *meso*-bound polycyclic aromatic ring to the *β* position of the porphyrin core. The fusion of covalently linked PAHs can be achieved via the Scholl reaction if the appropriate oxidant is used in conjunction with aromatic rings that are activated by electron-donating substituents.[29] The corresponding *β*,*meso*,*β* fusion of two or more porphyrins by Osuka et al. to form triply linked porphyrin tapes has been carried out using related oxidative fusion conditions.[12] There are only a few reports of the direct fusion of an unactivated aromatic group to a porphyrin core, all of which involve nickel(II)-based porphyrins.[15b,c,h] In most cases, activation of an aromatic ring by substitution with donor alkoxy or amino groups is required[15a,d−g] in addition to metalation of the porphyrin ring with nickel(II).[15a−c,e,g,h] The use of bulky donor substituents on the aromatic ring and the presence of nickel(II) significantly limits the scope of such reactions and is undesirable for applications in photovoltaics.[19] Unfortunately, the use of zinc(II)−metalated porphyrins and unactivated aromatic rings fails to give any fusion products under oxidative Scholl-type conditions.[15a,d]


dx.doi.org/10.1021/jo201490y | *J. Org. Chem.* 2012, 77, 143−159

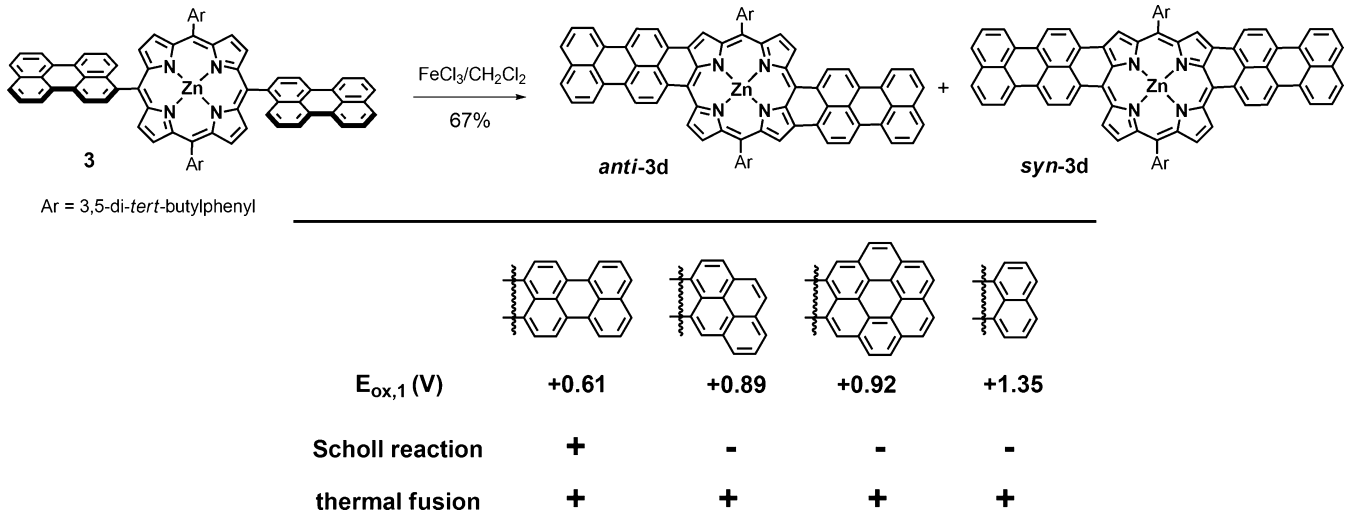


**Figure 1.** Scheme representing the products of the Scholl fusion reaction for **3** (top) and the success of polycyclic aromatic ring fusion to a porphyrin core by the Scholl reaction and under thermal conditions as a function of first oxidation potential of the aromatic ring ($E^{ox,1}$) versus $Fc^+/Fc$. A + sign indicates that the fusion reaction proceeds under the given conditions and a − sign indicates that no fused product was observed.

Previously, we reported the first example of fusion of unactivated pyrene rings to a porphyrin dimer metalated with zinc(II).[17] For this particular compound, the reaction is most likely favored by the low oxidation potential of the porphyrin dimer,[12] since the reaction cannot be extended to derivatives with a monoporphyrin core. Only the perylene rings in porphyrin **3** leads to a PAH fused porphyrin when **1**−**4** are treated to Scholl-type oxidative reaction conditions ($FeCl_3/CH_2Cl_2$) used for the fusion of unactivated pyrene rings to a porphyrin dimer (Figure 1).[17] Porphyrin **3** also undergoes demetalation during the oxidation process, so treatment with $Zn(OAc)_2$ is required to obtain the Zn(II) doubly fused porphyrin. This reaction gives an overall yield of 65−75%, affording a mixture of *syn* and *anti* regioisomeric porphyrins **3d** in a ca. 0.7:1 ratio (Figure 1). A number of reaction conditions have been used to attempt *β*,*meso* fusion of **2**, including $FeCl_3$,[15,17] $FeCl_3$/AgOTf,[15d,e] $Sc(OTf)_3$/DDQ,[15a,d−f] $PhI(OTf)_2/BF_3OEt_2$,[15a] (*p*-BrPh)$_3$NSbCl$_6$,[12a] and K/Na,[15a] however, none of these methods led to fused products.

The propensity for the aromatic ring to undergo *β*-fusion with the porphyrin using $FeCl_3$ can be correlated with the oxidation potential of the particular PAH. Perylene has the lowest oxidation potential among studied PAHs (0.61 V),[30] while the other extended aromatic systems studied here have higher oxidation potentials (≥0.89 V) (all potentials referenced to the ferrocenium/ferrocene couple).[30] For comparison, the oxidation potential of porphyrin **2** is 0.41 V. Thus, the ability of PAHs to fuse onto a porphyrin core in the Scholl reaction appears to depend on the oxidation potential of the aromatic groups, with the upper limit lying between the oxidation potential of perylene and pyrene rings. Alkoxy or amino activating groups act to lower the oxidation potentials of *meso*-aromatic groups and make them amenable to Scholl-type fusion reactions. The previous known example of fusion of a single perylene ring to a porphyrin core required the presence of an activating amino functionality,[15f] while our data demonstrates that fusion of two unsubstituted perylene rings can occur without the need of such an activating group.

Thermal activation of two or more C−H bonds in aromatic systems for direct C−C bond formation is known to proceed under the conditions of flash vacuum pyrolysis.[31] This reaction has been extensively studied as an efficient means to directly prepare polycyclic aromatics without the use of added reagents and solvents,[31] but such high temperature C−C bond forming reactions have not been studied in porphyrin chemistry. Porphyrins are thermally stable and relatively inert compounds; for example, **2** can be sublimed without decomposition at 430 °C in vacuum ($10^{-5}$ Torr). However, when sublimation is suppressed under an atmosphere of nitrogen, **2** undergoes thermal ring closure at elevated temperatures (500−530 °C) to afford singly (**2m**) or doubly fused (**2d**) porphyrins (Scheme 5). The product ratio (**2m**:**2d**) and reaction yield can be controlled by varying the reaction time. This reaction has also proven to be scalable, in excess of several grams, albeit with lower yields of **2d** (25−35%) and **2m** (7%). The major side product in large-scale reactions, comprising 35−40% of the porphyrinic material, involves the loss of either one or both of the di-*tert*-butylphenyl groups from **2d** depending on the reaction time. While the loss of the di-*tert*-butylphenyl group(s) reduces the yields of **2d**, the optical properties of the fused compounds are unaffected (see experimental part). To ensure that cyclodehydrogenation is not caused by the remaining impurities of palladium catalysts from the previous steps, a sample of **2** was extensively purified by column chromatography, crystallization and sublimation. The resultant high purity material undergoes thermal fusion under the same reaction conditions as the porphyrin purified by standard methods. Similarly, all of the attached aromatic rings can be fused in tetrakis(pyrenyl)porphyrin **5** to form the quadruply fused product **5t** as illustrated in Scheme 5, where only two isomers of the four possible isomers of **5t** are shown.

Thermal reactions in thin films of precursor materials have shown promise for scalable, efficient and inexpensive routes to electronic applications since it eliminates many preparation steps.[32] Usually, this is achieved by converting solution processable small molecule to insoluble organic semiconductor materials by thermal removal of leaving groups after fabrication of the film. This approach favors a face-to-face orientation of *π*-conjugated molecules, especially in such PAHs as the acenes, preventing formation of herringbone structures with undesired edge-to-face orientation. In practice, such reactions must be reliable, furnish high yields of the desired products, and proceed in the absence of external reagents and solvents. A good


dx.doi.org/10.1021/jo201490y | J. Org. Chem. 2012, 77, 143−159

**Scheme 5**

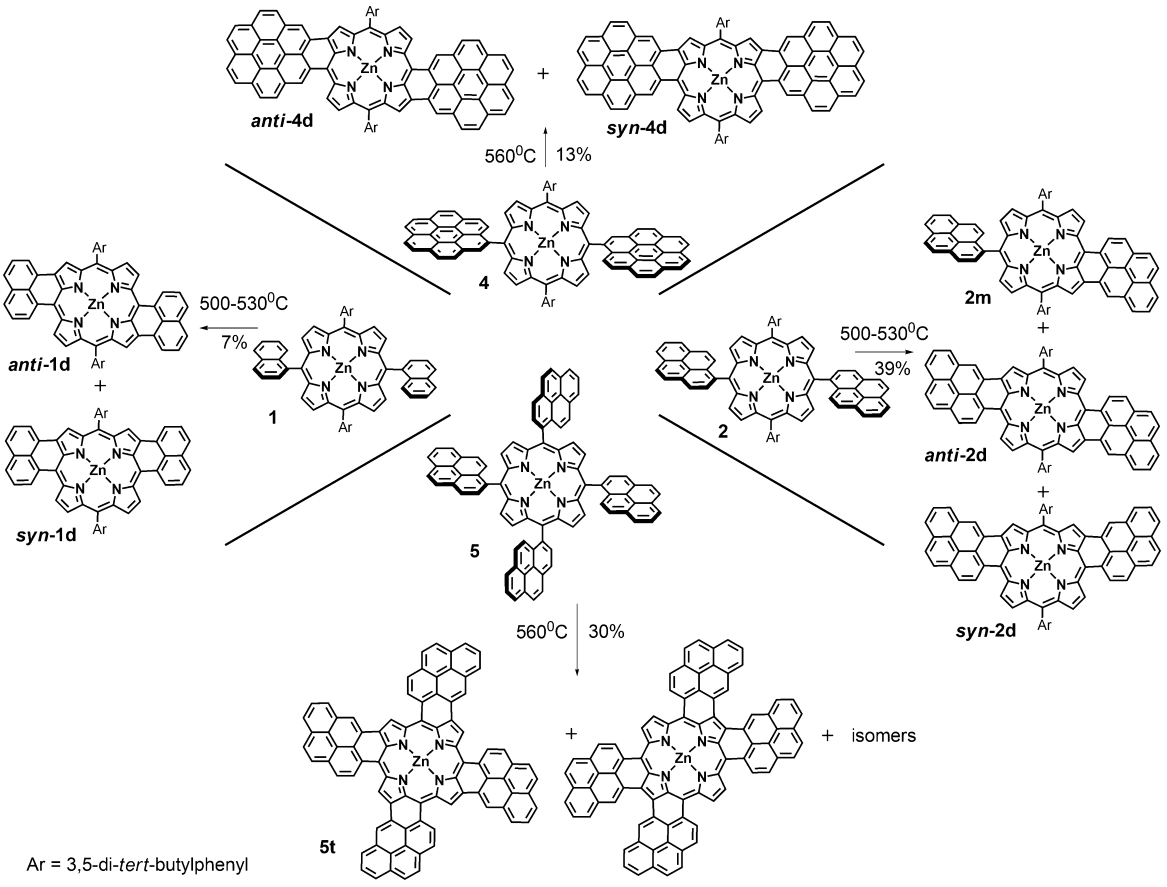


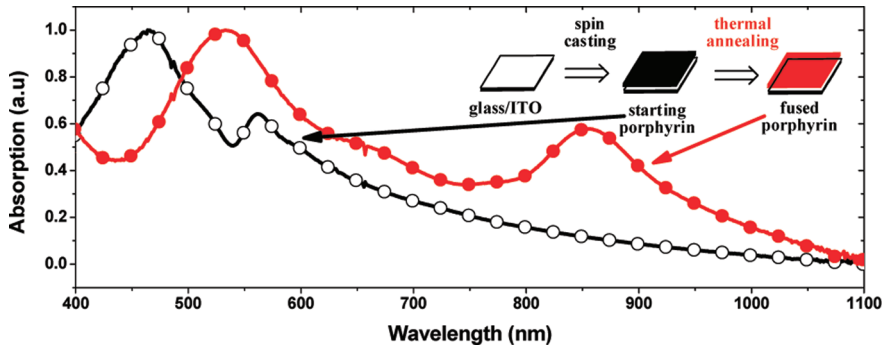


**Figure 2.** *In situ* fusion of porphyrin **2**. Film of compound **2** (500 Å) spin-cast on ITO from toluene solution and the same films after thermal annealing at 530 °C for 5 min.

example of such a process is the thermally promoted retro Diels–Alder reaction of soluble *β*,*β*-substituted porphyrin precursors to form an insoluble thin film of pure *β*,*β*-benzannulated tetrabenzopophyrin and four equivalents of ethylene gas.[33] This process was applied to thin film OPVs with various architectures.[32] Thermal cyclodehydrogenation of porphyrins substituted with *meso*-bound polycyclic aromatic rings represents a new approach for *in situ* preparation of materials that show good spectral coverage for applications where absorption in the NIR region is required, such as for OPVs and nonlinear optics.[9] Thermally annealing thin films or small amounts (50–100 mg) of **2** leads to complete conversion of the strong Soret band of the singly connected precursor into absorption peaks corresponding to only the doubly fused-products. Since the thermal fusion reaction proceeds in thin film form as it does in the bulk, the process is potentially suitable for *in situ* formation of graphene-like porphyrins on substrates (e.g indium–tin oxide) for applications in organic electronics (Figure 2). The formation of **2d** in the film can be monitored by the growth of a strong absorption band with $\lambda_{max}$ = 860 nm that is a signature of the fused product (*vide infra*). Thin films of **5t** were also obtained using a similar approach (Supporting Information). While this method can cleanly afford fused porphyrins, the resulting films have nanoscale pin-holes making them poor candidates for electronic devices. Further optimization of the conditions for thermal annealing as well as choice of the appropriate substrate may lead to pin-hole-free films.


dx.doi.org/10.1021/jo201490y | *J. Org. Chem.* 2012, 77, 143–159

The thermal cyclodehydrogenation reaction is not limited to porphyrins appended with *meso*-pyrenyl groups. Fusion can also be accomplished for *meso*-naphthalene and *meso*-coronenyl groups giving the doubly fused products **1d** and **4d** (Scheme 5), although yields are lower (10−13%) than for **2d**, due to losses during chromatographic separation and the formation of side products with the loss of di-*tert*-butyl-phenyl groups similar to those obtained in the thermal reaction of **2**. This data suggests that a thermal reaction should be possible for fusion of other PAHs to the porphyrin core as well.

The other metalated pyrene porphyrins **2-M** undergo similar fusion (Scheme 6), forming **2d-M**, (M = Mg, Cu, Pd, Pt), except for **2-Pb**, which leads to demetalated fused product.

**Scheme 6**

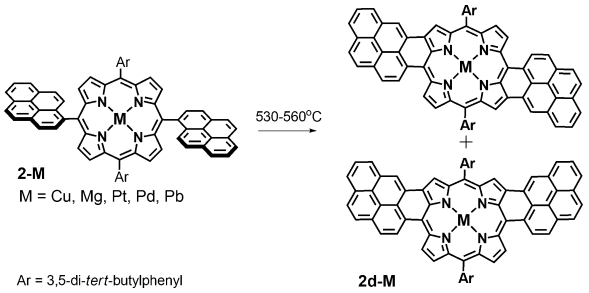


**Characterization.** The nonfused porphyrin precursors (**1**−**4** and **2-M**) and fused products (**1d**−**4d**, **2m**, **5t** and **2d-M**) were characterized using mass and NMR spectroscopy. The formation of ring fusion products is supported by the mass spectral data. For example, **2** gives a mass for the parent ion of 1149.4834 Da ($MH^+$), a loss of two hydrogens for **2m** ($[M]^+$ = 1146.4581 Da), and a loss of four hydrogens for **2d** ($[M]^+$ = 1144.4418 Da). Porphyrin **5** ($[MH]^+$ = 1173.2915 Da) shows a loss of eight hydrogens for **5t** ($[M]^+$ = 1164.32 Da) after thermal fusion. MALDI-TOF mass spectra of porphyrins **2m**, **2d** and **3d** obtained for samples without use of any matrices show the formation of molecular ions without significant fragmentation in the 20−5000 Da range indicating stability of the obtained fused porphyrins toward laser irradiation. The mass spectrum for fused porphyrin **4d** contains peaks of the molecular ion together with fragmentation products indicating the presence of fused products with the loss of one or both di-*tert*-butyl-phenyl groups. Both thermal (for **1**−**4**) and Scholl-type (for **3**) oxidative fusion leads to mixtures of *syn* and *anti* regioisomers. Regioisomers of doubly fused pyrenyl porphyrins *anti*-**2d** and *syn*-**2d** (1:1 ratio) can be separated using column chromatography. The regioisomers were structurally assigned using NMR spectroscopy on the basis of the number of equivalent di-*tert*-butylphenyl (Ar) groups. Regioisomer *anti*-**2d** has equivalent Ar groups (only one set of signals in NMR spectra), whereas the compound with inequivalent Ar groups (two independent sets of signals) is assigned to the *syn*-**2d** regioisomer. The size of $\pi$-system of porphyrin **4d** is close to that of the previously reported triply linked porphyrin trimers, which give extensive aggregation in solution.[12] The $^1$H NMR spectra of porphyrin **4d** contain only broad signals due to aggregation in solution, making its use for structural assignment impossible. The MALDI-TOF mass spectrum shows the parent ion as the base peak and subsequent peaks for loss of methyls from the di-*tert*-butyl-phenyl groups. Compound **4d** gives a higher level of fragmentation in its mass spectrum than other fused porphyrins, consistent with the fact that this compound requires a higher level of laser power to volatilize the compound than any of the other compounds reported here. The higher laser power is needed to overcome the cohesive forces in the films of **4d** due to strong intermolecular $\pi$−$\pi$ interactions between the pendent coronenes.

An important criterion in the design of appropriate candidates for thin film applications such as OPVs is the ease of processing (either by vacuum or solution deposition). Both $^1$H NMR data and molecular modeling (Figure 3; Supporting Information) suggest an out-of-plane distortion occurs in the $\beta$,*meso* fused porphyrins due to unfavorable interactions between $\alpha$ protons of the fused polycyclic aromatic ring and neighboring $\beta$-pyrrolic protons of the porphyrin rings (Figure 3). Such a structural distortion is known to improve solubility and processability in conjugated aromatics.[34] As a result, all fused porphyrins studied here are readily soluble in common organic solvents (benzene, toluene, etc.) and have high solubility in nonpolar solvents such as cyclohexane (ca. 1 mg/mL for **2d**). Even quadruply fused porphyrin **5t** is sufficiently soluble for NMR characterization. *Bis*-coronenyl fused porphyrin **4d** has the lowest solubility and the tendency to aggregate in solutions is similar to that of previously studied nondistorted porphyrin tapes.[12] Such high solubility is atypical for extensively fused aromatic compounds, even when appended with multiple solubilizing groups.[12,15]

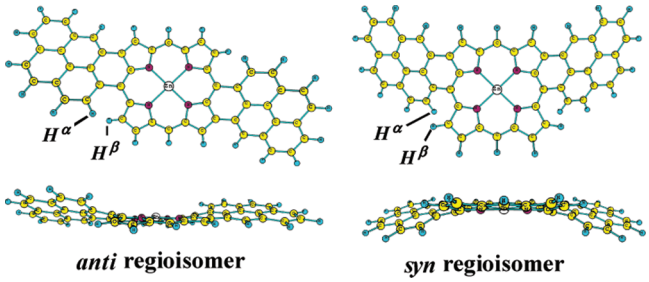


**Figure 3.** Structures of model porphyrins *anti*-**2d′** and *syn*-**2d′** calculated at B3LYP/6-31G*/LANL2DZ level.

**Electrochemical and Theoretical Characterization.** The electrochemical properties of zinc porphyrins **2**, **2m** and **2d** (*syn*/*anti* mixture) were analyzed using cyclic voltammetry (Table 1). Consistent with previous data,[15] the fused porphyrins show a significant decrease in the separation between $E^{ox}$ and $E^{red}$ potentials ($\Delta E^{ox\text{-}red}$). Compounds **2**, **2m** and **2d** give $\Delta E^{ox\text{-}red}$ values of 2.33, 1.70, and 1.45 V, respectively. The highest occupied (HOMO) and lowest unoccupied molecular orbital (LUMO) energy levels relative to vacuum for pyrenyl porphyrins **2**, **2m**, **2d** can be estimated

**Table 1. Electrochemical Potentials and Energy Levels[35] for the HOMO and LUMO Energies of Pyrene-functionalized Porphyrins 2, 2m and 2d[a]**

| compound | $E^{ox}$ | $E^{red}$ | $\Delta E^{ox\text{-}red}$ | $E^{HOMO}$ | $E^{LUMO}$ |
|---|---|---|---|---|---|
| **2** | 0.41 | −1.92 | 2.33 | 5.2 | 2.5 |
| **2m** | 0.18 | −1.52 | 1.70 | 4.8 | 3.0 |
| **2d** | 0.01 | −1.44 | 1.45 | 4.6 | 3.1 |

[a]Potentials were determined by cyclic voltammetry referenced to an internal ferrocenium/ferrocene potential. Each compound shows two oxidations and two reductions, but only the first oxidation and reduction values are listed.


dx.doi.org/10.1021/jo201490y | J. Org. Chem. 2012, 77, 143−159

from these electrochemical redox potentials, and are listed in Table 1.[35]

Theoretical calculations (B3LYP/6-31G*/LANL2DZ) performed on the model pyrenyl porphyrins without the di-*tert*-butylphenyl groups (**2′**, **2 m′**, *syn*-**2d′** and *anti*-**2d′**) also predict a decrease in the HOMO−LUMO gap ($\Delta E_{HL}$) with increasing degree of fusion. The calculated HOMO−LUMO gap for **2′** ($\Delta E_{HL}$ = 2.93 eV) decreases upon monofusion (**2 m′**, $\Delta E_{HL}$ = 2.19 eV), declines further upon double fusion (*syn*-**2d′**, $\Delta E_{HL}$ = 1.77; *anti*-**2d′**, $\Delta E_{HL}$ = 1.73 eV), and the values are consistent with the redox gaps determined electrochemically for **2**, **2m** and **2d**. As can be seen in a qualitative frontier molecular orbital diagram (Figure 4), the HOMO of the fused pyrenyl porphyrin

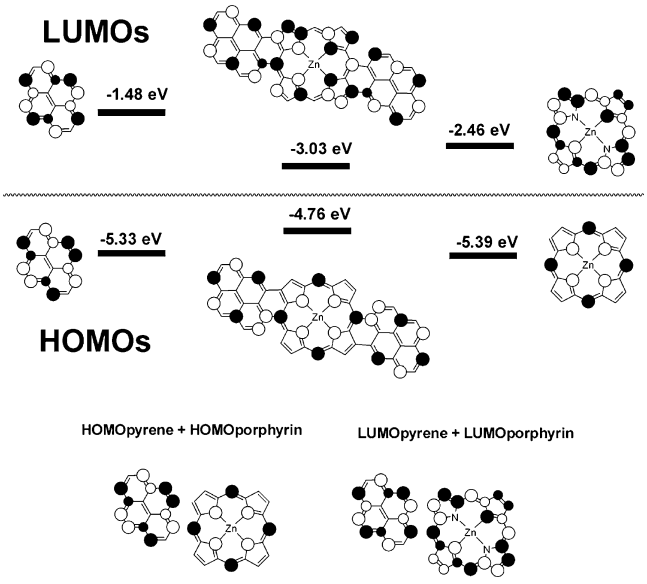


**Figure 4.** Qualitative frontier molecular orbital diagram of fused porphyrin *anti*-**2d′** as derived by B3LYP/6-31G*/LANL2DZ calculation.

consists of an out-of-phase combination of the corresponding HOMOs of pyrene and unsubstituted porphyrin rings, whereas the LUMO of the fused porphyrin is comprised of an in-phase combination of the corresponding LUMOs of the pyrene and porphyrin rings. This arrangement in the fused porphyrins leads to destabilization of the HOMO, stabilization of the LUMO, and a net decrease in the HOMO−LUMO gap.

AM1 method was used to calculate the structures and energies of model Zn porphyrins doubly fused with PAHs (Figure 5). The predicted HOMO−LUMO gaps for naphthyl

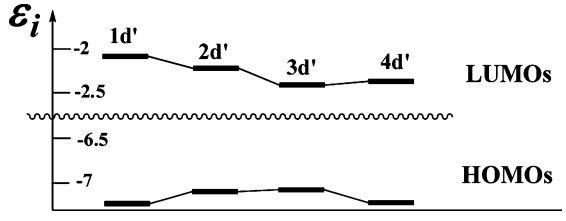


**Figure 5.** Energy diagram showing the LUMO and HOMO orbitals of different model Zn fused porphyrins calculated at the AM1 method. Structures of model porphyrins used for geometry optimizations have phenyl groups in place of the 3,5-di-*tert*-butylphenyl groups of **1d−4d**, and are abbreviated **1d′−4d′**.

**1d′**, pyrenyl **2d′**, perylenyl **3d′** and coronenyl **4d′** model porphyrins are consistent with the lowest-energy electronic transitions observed in fluid solution (*vide infra*). In particular, coronenyl derivative **4d′** has a larger energy gap compared with both **2d′** and **3d′** porphyrins. These calculations predict a progressive decrease in the HOMO−LUMO gap upon further increase in the size of the fused polycyclic aromatic, up to 16 condensed benzene units of the fused polycycle (see Supporting Information).

**Electronic Spectroscopy.** The absorption spectra for nonfused and fused porphyrins in solution are shown in Figures 6a−d, data are listed in the Experimental Section. The Soret bands in the parent porphyrins **1**, **2** and **4** appear as intense peaks at $\lambda_{max}$ = 430 nm (Figure 6a) with the Soret band of **4** split by 5 nm. Coronene itself has a relatively weak $S_0$−$S_1$ transition at 420 nm that is forbidden due to the $D_{6h}$ symmetry of a coronene core.[27] However, the lower symmetry of the coronene $\pi$-system in **4** causes this transition to be partially allowed. Compound **3** displays broad absorption bands centered at 425 and 460 nm, consistent with the Soret band and perylene $\pi$−$\pi^*$ transitions.

Upon pyrene ring fusion, the Soret bands in porphyrins **2m**, **2d** and **5t** undergo red-shifts to $\lambda_{max}$ = 490, 500−540, and 620 nm, respectively. The Soret bands in **2d** and **5t** also display peak splitting and broadening. Significant spectral changes are also observed for the Q bands (Figure 6b). The increased conjugation in porphyrins **2m**, *syn*-**2d**, *anti*-**2d**, and **5t** results in large bathochromic shifts of the Q-band to $\lambda_{max}$ = 706, 811, 815, and 890 nm, respectively, from $\lambda_{max}$ = 551 nm in **2**. Thus, the overall effect of multiple pyrene ring fusion in **5t** is a red shift of ca. 400−450 nm relative to **2** and **5**. Fusion with multiple pyrene rings also causes significant enhancement in the intensity of the Q-band relative to **2** (ca. 4 times in **2d**). Increased $\pi$-conjugation in perylenyl-fused porphyrin **3d** causes the Q-band to red-shift further up to $\lambda_{max}$ = 900 nm (Figure 6d). The absorption maximum of the Q-band in the various metalloporphyrins **2d-M** covers a significant portion of the NIR region, and undergoes a progressive blue-shift from $\lambda_{max}$ = 830 nm for **2d-Mg** to 740 nm for **2d-Pt** (Figure 6e).

Among the doubly fused compounds reported here, the coronenyl-fused porphyrin **4d** has the largest degree of $\pi$-extension, however, its absorption peak at 780 nm is significantly blue-shifted relative to the perylenyl porphyrin **3d** and also pyrenyl derivative **2d** (Figure 6d). The degree of orbital overlap between the PAH and the porphyrin core as well as the symmetries of the PAH orbitals in contact with the porphyrin core are the same for **1d−4d**. The ordering of the absorption band energies of the four fused porphyrin materials (i.e., **1d−4d**) appears to be related to the energies of the HOMO and LUMO orbitals of the PAH relative to those of the porphyrin core. Compound **2** is a good model for the porphyrin core frontier orbital energies, $E^{ox}$ = 0.41 V and $E^{red}$ = −1.92 V versus ferrocene; see Table 1. The oxidation and reduction potentials of the PAHs are given in Table 2 along with the energies of the Q bands for **1d−4d**. It is anticipated that PAHs with a frontier orbitals that lie closer in energy to those of the porphyrin core will undergo a greater degree of orbital mixing and thus destabilization for the HOMO and stabilization for LUMO in the fused porphyrin and will also display a larger bathochromic shift. Indeed, this is observed for **1d−4d**. Porphyrin **3d** has the best energy match for the porphyrin core and PAH frontier orbitals, and thus, the lowest energy Q-band. The energies of the frontier orbitals of coronene fall between those of naphthalene and perylene, and thus the energy of the Q-band in **4d** falls between **1d** and **3d**.

The relative intensities of the Soret and Q bands for the *β*,*meso*-fused porphyrins **1d−4d** appear to depend on the


dx.doi.org/10.1021/jo201490y | *J. Org. Chem.* 2012, 77, 143−159

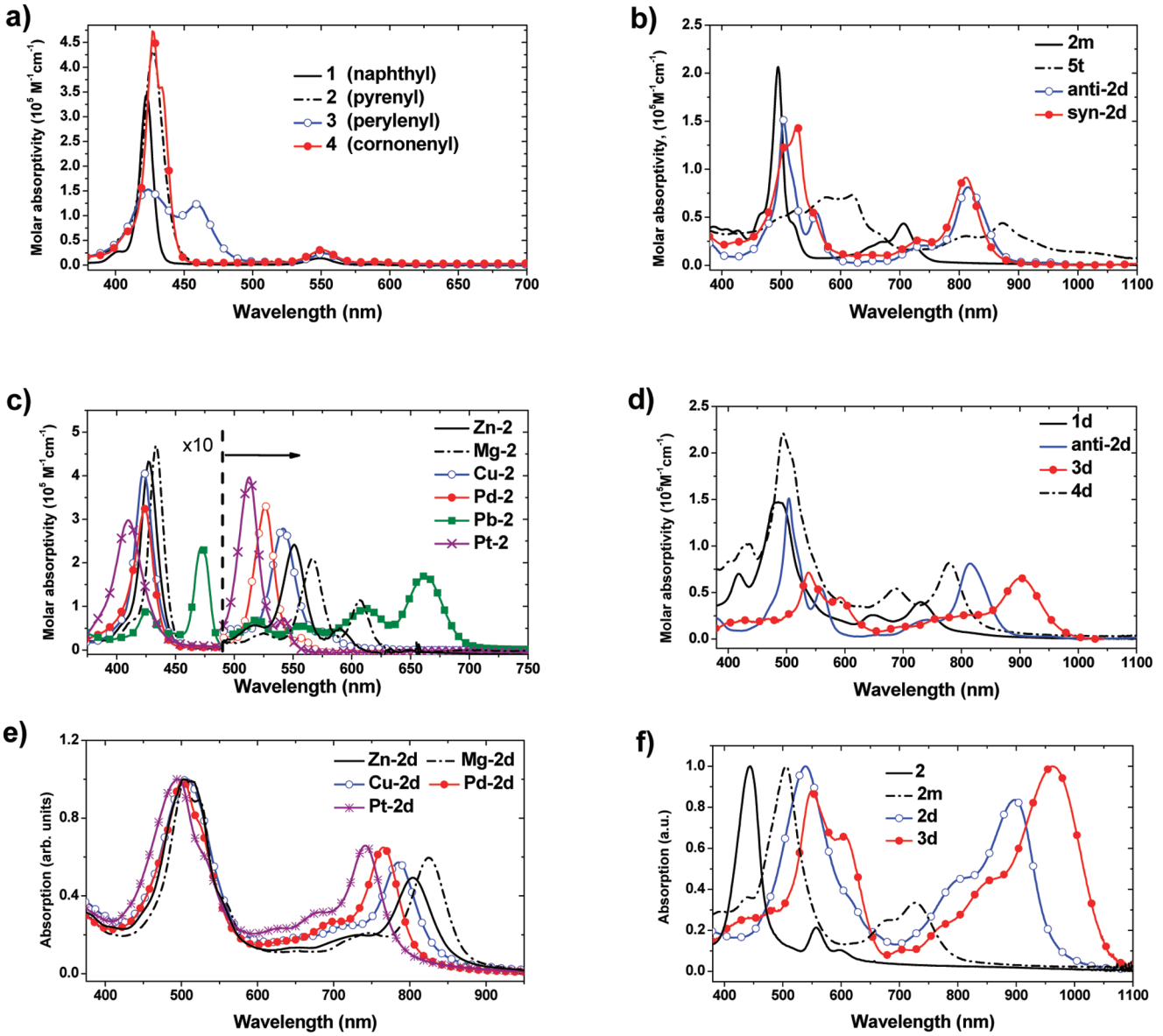


**Figure 6.** UV−vis absorption spectra of $CH_2Cl_2$ solutions of (a) porphyrins with *meso*-bound polycyclic aromatic rings **1**−**4**; (b) fused pyrenyl-porphyrins **2m**, ***anti*-2d**, ***syn*-2d**, and **5t** with 5% added pyridine; (c) metalated *bis*-pyrenyl-porphyrins **2-M**; (d) doubly fused porphyrins **1d**−**3d**, and **4d** with 5% added pyridine; (e) metalated doubly fused pyrenyl porphyrins **2d**, **Mg-2d**, dissolved directly after fusion at 530 °C and **Cu-2d**, **Pd-2d**, **Pt-2d** dissolved directly after fusion at 560 °C; (f) Absorption spectra of porphyrin **2** and fused porphyrins **2m**, **2d** and **3d** in spin-cast thin films.

difference in energies between the HOMO of the porphyrin ring and that of the respective PAHs. A close match between frontier orbital energies of the porphyrin and fused PAH give rise to Soret: Q-band intensities that approach 1:1 (Table 2). The intensity ratio of the Soret: Q-band for the aryl porphyrins is 17:1 for **2**, drops to 4:1 for the naphthyl fused porphyrin **1d**, and further to 1.1:1 for **3d**. Having Soret and Q bands of similar intensity is beneficial in designing OPVs or optical detectors, since this will give similar absorbance for both bands at any given film thickness.

**Table 2. Photophysical Data for Porphyrins 1d−4d and 2 and Electrochemical Data for Their Respective Polycyclic Aromatic Hydrocarbons (PAH)[a]**

| compound | 2 | 1d | 4d | 2d | 3d |
|---|---|---|---|---|---|
| Q-band wavelength (nm) | 550 | 730 | 780 | 815 | 900 |
| Soret: Q-band intensity | 17:1 | 4:1 | 2.8:1 | 1.6:1 | 1.1:1 |
| $E^{ox}/E^{red}$ of PAH[30] | | 1.35/−2.99 | 0.92/−2.53 | 0.89/−2.53 | 0.61/−2.14 |

[a]Electrochemical values are referenced to an internal ferrocenium/ferrocene couple in 0.1 M $Bu_4NPF_6$ in dichloromethane.

The absorption spectra for neat thin films of **2**, **2m**, **2d** and **3d** are shown in Figure 6f. The $\pi$-systems of the fused polycyclic aromatic moieties of the $\beta$,*meso*-fused porphyrins are not sterically hindered, making them accessible for $\pi-\pi$ interactions.[14,36] These $\pi-\pi$ interactions lead to significantly red-shifted absorptions in thin films of the fused porphyrins relative to their solution spectra (e.g., for the Q-band, the red shift is 85 nm for **2d** and 70 nm for **3d**). The bathochromic shift for the fused porphyrin **2d** is markedly larger (0.144 eV) than the shifts observed for thin films of unfused porphyrin **2** (0.024 eV), and also larger than for neat films of the previously reported pyrene-fused porphyrin dimer (0.078 eV).[17] This


dx.doi.org/10.1021/jo201490y | *J. Org. Chem.* 2012, 77, 143−159

bathochromic shift becomes more pronounced with increasing degree of fusion for a given PAH, for example, comparing the Q-band shifts of unfused porphyrn **2** (0.024 eV), to monofused **2m** (0.053 eV), to doubly fused **2d** (0.144 eV). This large bathochromic shift pushes absorption bands further into NIR than the $\pi$-extension alone, by utilizing $\pi-\pi$ interactions between fused PAHs with unhindered $\pi$-system. These shifts are also larger than what is observed in films of $\beta,\beta$ annulated tetrabenzo- and tetranaphthoporphyrins **PtTPBP** (0.039 eV) and **PtTPNP** (0.041 eV) (Scheme 7).

**Scheme 7**

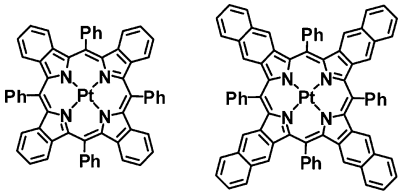


**PtTPBP** **PtTPNP**

Porphyrins **2**, **2m**, **2d** exhibit room temperature emission that undergoes red-shift with extending conjugation from 596 nm for **2** to 721, 829, and 839 nm for **2m**, *syn*-**2d** and *anti*-**2d**, respectively (Figure 7). The fluorescence quantum efficiencies

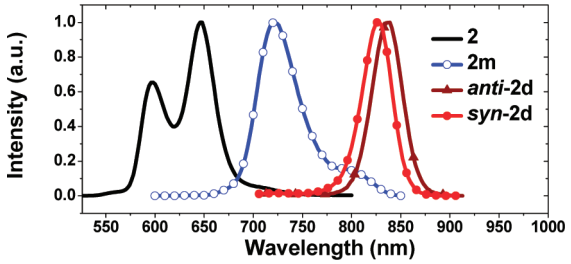


**Figure 7.** Fluorescence spectra of **2**, **2m**, *anti*-**2d** and *syn*-**2d** in $CH_2Cl_2$ at room temperature.

($\Phi_f$) increase from 3.3% for the starting nonfused porphyrin **2**, to 8% for the monofused porphyrin **2m**, to 8 and 13% for the doubly fused porphyrins *anti*-**2d** and *syn*-**2d**, respectively. This behavior is in contrast to what is expected from the energy gap law, which states that the nonradiative deactivation rate increases for related molecules as the $S_0-S_1$ energy gap decreases.[37] Such unexpected behavior may be due to the hindrance of vibrational deactivation modes by ring fusion. Many twisted acenes are known to exhibit strong fluorescence,[34b] suggesting that the distortion in fused porphyrins may also contribute to the increased fluorescence efficiency. The fluorescence efficiencies are comparable to those of the most efficient NIR-fluorescent porphyrin oligomers[11f] In contrast, closely related porphyrin tapes or directly linked $\beta$,*meso*-porphyrins have very low fluorescent efficiencies in the NIR ($\Phi_f = 10^{-5}$)[12d] due to very short $S_1$ excited state lifetimes.[12d,13]

**OPV Devices using 2d.** Porphyrins have been shown to act as donor and hole transporting materials in heterojunction OPVs.[2] Taking into account the energies and intensities of the absorption bands along with ease of synthesis, the doubly fused pyrenyl porphyrin **2d** was chosen as the best candidate for our initial OPV studies. The HOMO and LUMO of **2d** (Table 1) lie ca. 1.6 and 0.4 eV above the respective values of the fullerene acceptor $C_{60}$ ($E_{HOMO}$ = 6.2 eV, $E_{LUMO}$ = 3.5 eV).[3a] The energy offsets between **2d** and fullerene $C_{60}$ provide sufficient driving force for exciton separation for **2d** to act as donor material in an OPV using a $C_{60}$ acceptor layer (Figure 8b, inset). Thus,

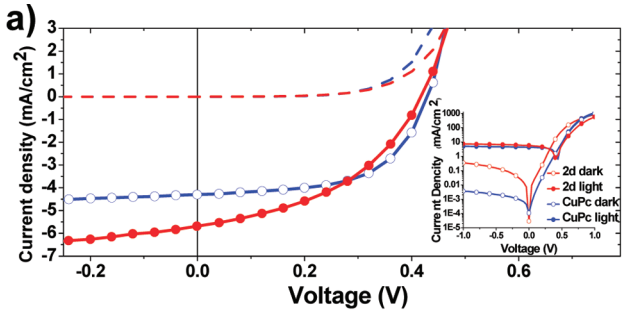


| Donor | $V_{oc}$ (V) | $J_{sc}$ (mA/cm$^2$) | FF | $\eta_p$ (%) |
|---|---|---|---|---|
| **2d** | 0.42 | 5.69 | 0.44 | 1.04 |
| CuPc | 0.43 | 4.30 | 0.58 | 1.08 |

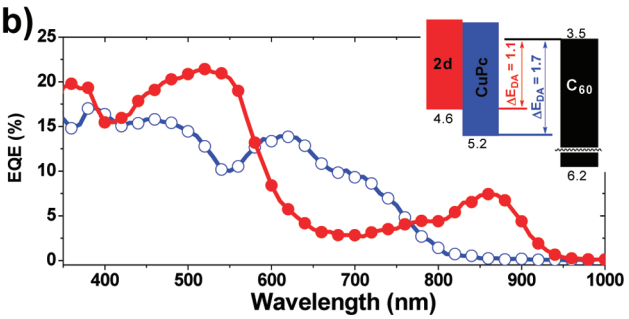


**Figure 8.** (a) I–V characteristics and performance metrics of ITO/donor/$C_{60}$(400 Å)/BCP(100 Å)/Al (1000 Å): donor layer = porphyrin **2d** (100 Å, red line, filled circles) and CuPc (400 Å, blue line, open circles); BCP = 2,9-dimethyl-4,7-diphenyl-1,10-phenanthroline, CuPc = copper phthalocyanine. (b) External quantum efficiency (EQE) as a function of wavelength for photovoltaic cells using porphyrin **2d** (red, filled circle) and CuPc (blue, open circle) donors. (Inset) Energy levels of **2d** and CuPc versus energy levels of fullerene as an acceptor. Energy levels for fullerene taken from ref 3a. HOMO level for **2d** calculated from electrochemical oxidation potentials.[35]

solar cells incorporating **2d** were fabricated using a structure: ITO/**2d**(100 Å)/$C_{60}$(400 Å)/BCP(100 Å)/Al(1000 Å), similar to that used for a copper phthalocyanine (CuPc)/$C_{60}$ reference cell and related porphyrin based cells.[3a,b] The current density versus voltage (J–V) characteristics were measured in the dark (dashed lines) and under simulated 1 sun (1 kW/m$^2$) AM1.5G illumination (circles).[38] Efficiencies were determined after correction for spectral mismatch between the xenon source lamp and ASTM G173–03 global.[39] Overall, thin layers (100 Å) of thermally evaporated porphyrin **2d** yield a power conversion efficiency (PCE = 1.04%), which is close to that of the reference (CuPc, 400 Å/$C_{60}$) device (PCE = 1.08%). Surprisingly, even though the $\Delta E_{DA}$ values suggest the OPVs based on **2d** should give a lower open circuit voltage ($V_{oc}$) than those with a CuPc donor, the open circuit voltage of porphyrin


dx.doi.org/10.1021/jo201490y | J. Org. Chem. 2012, 77, 143–159

**2d**/$C_{60}$ based OPV ($V_{oc}$ = 0.42 V) and CuPc/$C_{60}$ based OPV ($V_{oc}$ = 0.43 V) are very close. Studies of OPVs with the other fused-PAH porphyrins reported here are beyond the scope of this paper and will be reported elsewhere.

## CONCLUSIONS

Functionalization of the *meso* positions of porphyrins with polycyclic aromatic rings can be accomplished in relatively large scale by Suzuki coupling starting from available building blocks. Fusion of the resulting porphyrins using Scholl-type oxidative conditions has been extensively studied for further ring closure of the aromatic systems to the porphyrin core. Prior literature examples of such fusion to a monoporphyrin core require either substitution of PAHs with donor alkoxy or amino- groups or metalation of porphyrins with nickel. Here we demonstrate that neither donor groups at PAHs nor metalation with nickel is needed to for the formation of porphyrins *β,meso*-fused with PAHs. To overcome limitations of the Scholl reaction in fusing unactivated aromatic rings, a new thermal method has been developed. We have shown that *β,meso*-fusion of aromatic groups at one, two or all four *meso* positions of a porphyrin core can be accomplished using a thermal ring-closure reaction. For pyrenyl-substituted porphyrins thermal method gives synthetically acceptable yields of fused porphyrins (>30%). Further optimization of thermal conditions by surface assisted cyclodehydrogenation can potentially lead to higher yields of fused porphyrins. This fusion reaction does not require activation of the porphyrins using an appropriate metal or an aromatic group with donor substituents and has significant potential for further development of high-temperature reactions involving porphyrins and potentially other porphyrinoid macrocycles.

Porphyrin **2d** has a high extinction and emits with a quantum efficiency of 13% within biological window. All of the fused porphyrins reported exhibit enhanced solubility relative to their nonfused precursors, making them promising for organic electronics applications. The π-systems of the fused polycyclic aromatic moieties of the *β,meso*-fused porphyrins are not sterically hindered, allowing for accessibility to π−π interactions with a large bathochromic shift of the Q-band up to 0.144 eV for **2d**. Based on a number of material criteria, pyrene porphyrin **2d** was chosen for use in OPVs. Devices incorporating **2d** as a donor show high EQE response in the NIR (up to 950 nm), resulting in high $J_{SC}$, while having open-circuit voltages comparable to that of analogous CuPc devices. Our results suggest that these systems will be of broad interest as NIR dyes for organic photovoltaic devices, two-photon absorption, nonlinear optics, bioimaging and photodynamic therapy.

## EXPERIMENTAL SECTION

**1. General.** All reagents and solvents are commercial reagent grade and were used without further purification including anhydrous iron(II) chloride, dry dichloromethane, coronene, perylene, naphthalene-1-boronic acid, pyrene-1-boronic acid, 1-pyrenecarboxaldehyde. Starting [5,15-*bis*-(3,5-di-*tert*-butylphenyl)porphyrinato(2-)]zinc(II)[40] was prepared from dipyrromethane[25c] and 3,5-di-*tert*-butylbenzaldehyde[41] by known methods. [10,20-*Bis*-(3,5-di-*tert*-butylphenyl)-5,15-*bis*-bromoporphyrinato(2-)]zinc(II) was prepared by bromination of [5,15-*bis*-(3,5-di-*tert*-butylphenyl)porphyrinato(2-)]zinc(II) with NBS in 5%-pyridine/dichloromethane according to literature. Starting 4,4,5,5-tetramethyl-2-(naphth-1-yl)-1,3,2-dioxaborolane[42] and 4,4,5,5-tetramethyl-2-(pyren-1-yl)-1,3,2-dioxaborolane[43] were obtained from the corresponding boronic acids and pinacol (Method B, *vide infra*). Starting 4,4,5,5-tetramethyl-2-(pyren-1-yl)-1,3,2-dioxaborolane,[43] 4,4,5,5-tetramethyl-2-(perylen-1-yl)-1,3,2-dioxaborolane[45] and 4,4,5,5-tetramethyl-2-(coronen-1-yl)-1,3,2-dioxaborolane were obtained from the corresponding bromides and pinacolborane (Method A, *vide infra*). Moisture or air sensitive reactions were performed under an inert atmosphere of nitrogen. Flash chromatography was carried out with silica gel (60−200 mesh) and alumina (neutral, activity grade I). $^1$H NMR spectra were measured at either 400 or 600 MHz and are reported with chemical shifts as the delta scale in ppm relative to the residual nondeuterated solvent $CHCl_3$ (δ 7.26 ppm) or $C_6H_6$ (δ 7.15 ppm). Coupling constants (*J*) are given in Hz. $^{13}$C NMR spectra were proton wide-band decoupled and chemical shifts were reported as the delta scale in ppm relative to $CHCl_3$ (δ 77.0 ppm) or $C_6D_6$ (δ 128.02 ppm). MALDI-TOF mass spectra were recorded using a positive-MALDI-TOF method with/without α-cyano-4-hydroxycinnamic acid (CHCA) matrix. All spectra were measured as solutions in the indicated solvents at room temperature using a 1 cm cell. Absorption maxima ($\lambda_{max}$) are reported in nm and extinction coefficients (ε) in $M^{-1}cm^{-1}$. Quantum efficiency measurements were carried out using a system equipped with a xenon lamp, calibrated integrating sphere and photonic multichannel analyzer. Redox potentials were measured by the cyclic voltammetry method and differential pulse voltammetry method. 0.1 M *n*-$Bu_4NPF_6$ in $CH_2Cl_2$ was used as the supporting electrolyte (degassed with nitrogen), a Pt wire was employed as the counter electrode, an Ag wire used as the pseudoreference electrode and a glassy carbon electrode was used as the working electrode. Ferrocene (Fc) or decamethylferrocene (dmfc) was added as an internal reference, and the potentials were measured relative to the $Fc/Fc^+$ couple. CV was used to determine electrochemical reversibility, while all redox potentials were found using DPV.

*[5,15-Bis-(3,5-di-tert-butylphenyl)porphyrinato(2-)]zinc(II).*[40] Trifluoroacetic acid (3 mL) was added to a stirred solution of 3,5-di-*tert*-butylbenzaldehyde (8.72 g, 39.8 mmol) and dipyrromethane (5.85 g, 39.8 mmol) in dichloromethane (5 L) under nitrogen atmosphere and the reaction mixture was stirred at ambient temperature for 3 h. After that, DDQ (13.4 g, 60.4 mmol) was added and stirring continued for additional 30 min. The reaction mixture was quenched with triethylamine (15 mL) and passed through filter (2 L) filled with silica gel (800 g) washing with dichloromethane. All purple fractions were collected, dichloromethane was evaporated to a volume of 500 mL. To this solution of the corresponding free-base porphyrin, 30 mL of saturated solution of zinc(II) acetate in methanol was added and the resulting mixture was stirred for 3 h at ambient temperature. The reaction mixture was washed with water, and dichloromethane solution was passed through filter filled with silica gel (200 g) washing with dichloromethane. The residue after evaporation of solvents was crystallized from dichloromethane by adding methanol to give [5,15-*bis*-(3,5-di-*tert*-butylphenyl)porphyrinato(2-)]zinc(II) (7.46 g, 9.95 mmol, 50%). Characterization is given in reference 40.

*[10,20-Bis-(3,5-di-tert-butylphenyl)-5,15-bis-(1-naphthyl)-porphyrinato(2-)]zinc(II)* ***1***. (A) NBS (5 g, 28 mmol, 2.1 equiv.) was added to a stirred solution of [5,15-*bis*-(3,5-di-*tert*-butylphenyl)-porphyrinato(2-)]zinc(II) (10 g, 13.33 mmol) in dichloromethane (700 mL) and pyridine (20 mL) at −10 °C (NaCl/ice bath) under nitrogen atmosphere. The reaction mixture was stirred at the same temperature for 10 min, after that allowed to warm to 0 °C (ca. 5 min, water bath) and then quenched with acetone (20 mL). The crude reaction mixture was passed through short silica gel column, eluting with dichloromethane−pyridine mixture (100:1). All green-purple fractions were collected, the solvents were evaporated, the residue was dissolved in dichloromethane−pyridine mixture (95:5, 100 mL) and 200 mL of methanol was added to precipitate bromoporphyrin. All crystals were collected by filtration after 30 min to give [10,20-*bis*-(3,5-di-*tert*-butylphenyl)-5,15-*bis*-bromo-porphyrinato(2-)]zinc-(II)[11e,24a] (10.5 g, 11.6 mmol, 87%).

(B) A mixture of the above dibromoporphyrin (1.13 g, 1.25 mmol), cesium carbonate (4.2 g, 12.9 mmol, 11 equiv.), $Pd(PPh_3)_4$ (130 mg, 10 mol %), pyridine (3 mL) and 4,4,5,5-tetramethyl-2-(naphth-1-yl)-1,3,2-dioxaborolane[42] (0.73 g, 2.87 mmol, 2.3 equiv) in toluene (200 mL) was degassed and refluxed under nitrogen for 12 h. Reaction mixture was cooled and passed consecutively through pads of silica gel and neutral alumina washing with toluene. Toluene was distilled off in vacuum, the residue was separated by crystallization from dichloromethane by


dx.doi.org/10.1021/jo201490y | J. Org. Chem. 2012, 77, 143−159

adding methanol to afford [10,20-*bis*-(3,5-di-*tert*-butylphenyl)-5,15-*bis*-(naphth-1-yl)porphyrinato(2-)]zinc(II) **1** (*MeOH complex, 1.08 g, 1.047 mmol, 93%). $^1$H NMR ($CDCl_3$, 500 MHz): 1.52 and 3.05 (s, 36H), 7.11 (t, 2H, $J$ = 7.5 Hz), 7.20 (dd, 2H, $J^1$= 8.5; $J^2$= 14.5 Hz), 7.49 (t, 2H, $J$ = 7.5 Hz), 7.78 (s, 2H), 7.88 (t, 2H, $J$ = 7.5 Hz), 8.07 and 8.11 (s, 4H, atropoisomers), 8.29 (d, 2H, $J$ = 8.5 Hz), 8.33 (dd, 2H, $J^1$= 3 Hz, $J^2$= 6 Hz). $^{13}$C NMR ($CDCl_3$, 125 MHz): 29.7, 31.7, 35.0, 118.2, 120.7, 122.4, 124.1, 125.5, 126.0, 127.8, 128.3, 128.87, 128.90, 129.6, 129.8, 129.9, 131.7, 132.4, 132.5, 132.6, 132.8, 136.9, 140.3, 141.7, 148.47, 148.49, 148.51, 150.52, 150.7. UV/vis ($CH_2Cl_2$) $\lambda$, nm, ($\varepsilon$): 308 (8073), 345 (6074), 423 (345474), 511 (1472), 549 (14142), 588 (1595). HRMS: 1000.4419 ($M^+$ and $MH^+$), calcd. 1000.4417 for $C_{68}H_{64}N_4Zn$.

*4,4,5,5-Tetramethyl-2-(pyren-1-yl)-1,3,2-dioxaborolane.*[17,43] (Method A) To a ca. 0.1 M solution of 1-bromopyrene in toluene 10 mol % of $Cl_2Pd(PPh_3)_2$, 5 equivalents of pinacolborane and 10 equivalents of triethylamine were added. Reaction mixture was degassed with nitrogen and refluxed overnight. Reaction mixture was quenched with water, toluene was distilled off and the residue was subjected to column chromatography on silica gel (gradient elution with hexanes − ethyl acetate mixtures from 1:0 to 1000:5) to give 70−80% of 4,4,5,5-tetramethyl-2-(pyren-1-yl)-1,3,2-dioxaborolane. $^1$H NMR ($CDCl_3$, 400 MHz): 1.51 (s, 12H), 8.02 (t, 1H, $J$ = 7.7 Hz), 8.07−8.24 (m, 6H), 8.56 (d, 1H, $J$ = 9.7 Hz), 9.09 (d, 1H, $J$ = 9.7 Hz). MALDI TOF: 328 ($M^+$), requires 328.16 for $C_{22}H_{21}BO_2$.

(Method B). According to reference 44. A mixture of commercially available 1-pyreneboronic acid (10 g, 40.7 mmol) and pinacol (5.8 g, 49 mmol, 1.2 equiv) in ether (200 mL) and dichloromethane (600 mL) was stirred at ambient temperature for 1 day. Evaporation of solvents gave crude 4,4,5,5-tetramethyl-2-(pyren-1-yl)-1,3,2-dioxaborolane which was used for the next step without further purification.

*[10,20-Bis-(3,5-di-tert-butylphenyl)-5,15-bis-(1-pyrenyl)-porphyrinato(2-)]zinc(II).*[17] **2.** A mixture of the above dibromoporphyrin (6.33 g, 6.98 mmol), cesium carbonate (23.5 g, 70 mmol, 10 equiv.), $Pd(PPh_3)_4$ (800 mg, 10 mol %), pyridine (10 mL) and the 4,4,5,5-tetramethyl-2-(pyren-1-yl)-1,3,2-dioxaborolane (5.26 g, 16.03 mmol, 2.3 equiv) in toluene (800 mL) was degassed and refluxed under nitrogen for 12 h. Reaction mixture was cooled and passed consecutively through pads of Celite, silica gel and neutral alumina washing with toluene. Toluene was distilled off in vacuum, the residue was separated by crystallization from dichloromethane by adding methanol to afford [10,20-*bis*-(3,5-di-*tert*-butylphenyl)-5,15-*bis*-(1-pyrenyl)porphyrinato(2-)]zinc(II) **2** (*MeOH complex, 6.2 g, 5.25 mmol, 75%). $^1$H NMR ($CDCl_3$, 400 MHz): 1.47, 1.477 and 1.481 (s, 36H, atropoisomers), 7.50 (dd, 2H, $J$ = 9.3, 10.6 Hz), 7.71−7.74 (m, 4H, atropoisomers), 8.04−8.14 (m, 8H), 8.33 (t, 4H, $J$ = 7.2 Hz), 8.42 (d, 2H, $J$ = 9.1 Hz), 8.54 (d, 2H, $J$ = 7.7 Hz), 8.63 (dd, 4H, $J$ = 0.8, 4.7 Hz), 8.86 (dd, 2H, $J$ = 2.8, 7.7 Hz), 8.92 (d, 4H, $J$ = 4.7 Hz). $^{13}$C NMR ($CDCl_3$, 100 MHz): 31.7, 35.0, 118.9, 120.8, 122.7, 122.8, 124.1, 124.7, 125.2, 125.5, 126.2, 127.4, 127.5, 127.7, 127.9, 129.6, 129.8, 129.9, 130.8, 131.3, 131.8, 132.0, 132.5, 132.6, 132.64, 133.4, 133.5, 137.9, 141.6, 148.6, 150.7, 151.0. UV/vis ($CH_2Cl_2$) $\lambda$, nm, ($\varepsilon$): 235 (84899), 243 (120670), 264 (48136), 275 (69032), 308 (34871), 323 (47186), 337 (54350), 427 (432531), 517 (6415), 551 (24905), 590 (5614). HRMS: 1149.4834 ($M^+$ and $MH^+$), calcd. 1149.4808 for $C_{80}H_{69}N_4Zn$. MALDI TOF: 1150 ($M^+$ and $MH^+$), requires 1149.48 for $C_{80}H_{69}N_4Zn$. Elemental analysis for $C_{80}H_{68}N_4Zn$*MeOH: calcd C 82.25, H 6.14, N 4.74; found C 82.45, H 6.25, N 4.65.

*[10,20-Bis-(3,5-di-tert-butylphenyl)-5,15-bis-(perylen-1-yl)-porphyrinato(2-)]zinc(II)* ***3.*** A mixture of the above dibromoporphyrin (3.4 g, 3.75 mmol), cesium carbonate (12.6 g, 39 mmol, 10 equiv), $Pd(PPh_3)_4$ (430 mg, 10 mol %), pyridine (5 mL) and 4,4,5,5-tetramethyl-2-(perylen-1-yl)-1,3,2-dioxaborolane[45] (3.12 g, 8.25 mmol, 2.2 equiv) in toluene (200 mL) was degassed and refluxed under nitrogen for 15 h. Reaction mixture was cooled and passed consecutively through pads of silica gel and neutral alumina washing with dichloromethane. Solvents were distilled off in vacuum, the residue was separated by crystallization from dichloromethane to afford [10,20-*bis*-(3,5-di-*tert*-butylphenyl)-5,15-*bis*-(perylen-1-yl)-porphyrinato(2-)]zinc(II) **3** (1.54 g, 1.23 mmol, 33%). $^1$H NMR (5% pyridine-$d_5$ in $CDCl_3$, 500 MHz): 1.415 and 1.422 (s, 36H), 6.84 (dd, 2H, $J^1$= 8.5 Hz, $J^2$= 18 Hz), 8.92 (dd, 2H, $J^1$= 8.5 Hz, $J^2$= 16 Hz), 7.50 (t, 2H, $J$ = 8 Hz), 7.56 (t, 2H, $J$ = 7.5 Hz), 7.60 and 7.67 (t, 2H, $J$ = 1.5 Hz, atropoisomers), 7.73 (t, 4H, $J$ = 8.5 Hz), 7.93, 8.00, and 8.05 (d, 4H, $J$ = 1.5 Hz, atropoisomers), 8.10−8.12 (m, 2H), 8.22−8.26 (m, 2H), 8.42 (d, 2H, $J$ = 7.5 Hz), 8.51 (d, 2H, $J$ = 7.5 Hz), 8.69 (dd, 4H, $J^1$= 2 Hz, $J^2$= 4.5 Hz), 8.80 (d, 4H, $J$ = 4.5 Hz). $^{13}$C NMR could not be acquired due to low solubility of **3**. UV/vis ($CH_2Cl_2$) $\lambda$, nm, ($\varepsilon$): 257 (53872), 424 (152871), 459 (123061), 552 (23698), 591 (6611). HRMS: 1248.5001 ($M^+$ and $MH^+$), calcd. 1248.5043 for $C_{88}H_{72}N_4Zn$.

*4,4,5,5-Tetramethyl-2-(coronen-1-yl)-1,3,2-dioxaborolane.* A) Coronene (1.9 g, 6.33 mmol) was dissolved in 600 mL of chlorobenzene in dark at 70−80 °C. Higher temperature is required to completely dissolve coronene. Bromine (5.5 g, 34.8 mmol, 5 equiv) was added at once and the mixture stirred for 5−10 min. After that, reaction mixture was cooled down and the precipitate was filtered and washed with chlorobenzene to afford a mixture of bromocoronenes (2 g). MALDI TOF: bromocoronene, 378.17 ($M^+$), requires 378.00 for $C_{24}H_{11}Br$; dibromocoronene, 456.08 ($M^+$), requires 455.91 for $C_{24}H_{10}Br_2$. This mixture was used for the next step without further purification.

B) The mixture of bromocoronenes (2 g) from the previous step, HB(pin) (6 mL), $Cl_2Pd(PPh_3)_2$ (0.4 g) in toluene (150 mL) and triethylamine (25 mL) was refluxed overnight, cooled down to room temperature and the excess of HB(pin) quenched with slow addition of methanol (2 mL). The residue after evaporation of solvents in vacuum was subjected to column chromatography on silica gel by using mixture of dichloromethane−hexanes as eluent. The first fraction (dichloromethane−hexanes = 1:9) contained 4,4,5,5-tetramethyl-2-(coronen-1-yl)-1,3,2-dioxaborolane, the second fraction (dichloromethane−hexanes = 1:9) contained a mixture of isomeric *bis*-(4,4,5,5-tetramethyl-1,3,2-dioxaborolan-2-yl)coronenes.

*4,4,5,5-Tetramethyl-2-(coronen-1-yl)-1,3,2-dioxaborolane.* Yield 140 mg (0.33 mmol, 7%). The yield depends on the ratio of monobromocoronene in the mixture of bromocoronenes and can be increased to 15% by using less amount of bromine, however separation of the products turned to be more difficult due to the presence of unreacted coronene in the mixture. $^1$H NMR ($CDCl_3$, 500 MHz): 1.66 (s, 12H), 8.76−8.79 (m, 7H), 8.87 (dd, 2H, $J^1$= 2 Hz, $J^2$= 8.5 Hz), 9.48 (s, 1H), 9.80 (d, 1H, $J$ = 8.5 Hz). $^{13}$C NMR ($CDCl_3$, 100 MHz): 25.2, 84.2, 122.20, 122.22, 122.3, 122.4, 122.5, 124.1, 125.7, 125.9, 125.92, 126.0, 126.1, 126.2, 126.46, 126.52, 126.9, 127.6, 128.3, 128.4, 128.5, 129.3, 132.2, 136.1. HRMS: 426.1781 ($M^+$), calcd. 426.1786 for $C_{30}H_{23}BO_2$.

*1,7-Bis-(4,4,5,5-tetramethyl-1,3,2-dioxaborolan-2-yl)coronene.* The mixture of bis-B(pin)coronenes (the second fraction after column chromatography) was separated further by fractional crystallization from dichloromethane by adding methanol. The first collected portion of crystals can be identified as symmetric 1,7-bis-B(pin)-coronene due to simplicity of $^1$H NMR spectrum. Yield, 300 mg (0.54 mmol). $^1$H NMR ($CDCl_3$, 500 MHz): 1.63 (s, 24H), 8.90−8.95 (m, 6H), 8.53 (s, 2H), 9.88 (d, 2H, $J$ = 8.5 Hz). HRMS: 552.2654 ($M^+$), calcd. 552.2638 for $C_{36}H_{34}B_2O_4$.

*[10,20-Bis-(3,5-di-tert-butylphenyl)-5,15-bis-(coronen-1-yl)-porphyrinato(2-)]zinc(II)* ***4.*** A mixture of the above dibromoporphyrin (140 mg, 0.155 mmol), cesium carbonate (520 mg, 10 equiv), $Pd(PPh_3)_4$ (30 mg, 17 mol %), pyridine (1 mL) and 4,4,5,5-tetramethyl-2-(coronen-1-yl)-1,3,2-dioxaborolane (132 mg, 0.301 mmol, 2 equiv) in toluene (100 mL) was degassed and refluxed under nitrogen for 20 h. Toluene was distilled off in vacuum, the residue was separated on silica gel column by using a mixture of dichloromethane−hexanes as eluent. The first fraction (dichloromethane−hexanes = 1:9) contained mono-coronenylporphyrin [10,20-*bis*-(3,5-di-*tert*-butylphenyl)-5-(coronen-1-yl)porphyrinato(2-)]zinc(II). The second fraction (dichloromethane−hexanes = 3:9 to dichloromethane−pyridine = 100:1) contained [10,20-*bis*-(3,5-di-*tert*-butylphenyl)-5,15-bis-(coronen-1-yl)-porphyrinato(2-)]zinc(II) **4**. Each fraction was crystallized from dichloromethane by layered addition of methanol.

*[10,20-Bis-(3,5-di-tert-butylphenyl)-5-(coronen-1-yl)-porphyrinato(2-)]zinc(II).* Yield 15 mg (0.0144 mmol, 9%). $^1$H NMR


dx.doi.org/10.1021/jo201490y | J. Org. Chem. 2012, 77, 143−159

($CDCl_3$, 500 MHz): 1.51 (s, 18H), 1.512 (s, 18H), 7.77 (t, 2H, $J$ = 1.5 Hz), 8.13 (t, 2H, $J$ = 1.5 Hz), 8.16 (t, 2H, $J$ = 1.5 Hz), 8.21 (d, 1H, $J$ = 9 Hz), 8.50 (d, 1H, $J$ = 9 Hz), 8.70 (d, 2H, $J$ = 4.5 Hz), 8.81 (d, 1H, $J$ = 9 Hz), 8.93 (d, 2H, $J$ = 4.5 Hz), 8.95 (d, 1H, $J$ = 8.5 Hz), 8.99–9.08 (m, 5H), 9.11 (d, 1H, $J$ = 8.5 Hz), 9.20 (d, 2H, $J$ = 4.5 Hz), 9.48 (d, 2H, $J$ = 4.5 Hz), 9.75 (s, 1H), 10.37 (s, 1H). $^{13}$C NMR ($CDCl_3$, 150 MHz): 29.7, 31.73, 35.0, 106.3, 118.9, 120.8, 122.0, 122.3, 122.8, 122.9, 123.1, 126.2, 126.3, 126.34, 126.42, 126.49, 126.50, 126.6, 127.0, 127.2, 128.4, 129.0, 129.1, 129.7, 129.9, 131.7, 132.1, 132.5, 132.59, 132.61, 133.0, 134.3, 139.9, 141.5, 148.62, 148.64, 149.9, 150.8, 151.37, 151.4. HRMS: 1047.4358 ($M^+$ and $MH^+$), calcd. 1047.4339 for $C_{72}H_{63}N_4Zn$.

*[10,20-Bis-(3,5-di-tert-butylphenyl)-5,15-bis-(coronen-1-yl)-porphyrinato(2-)]zinc(II)* ***4***. Yield 117 mg (0.0869 mmol, 56%). $^1$H NMR (5% pyridine-$d_5$ in $CDCl_3$, 600 MHz): 1.38, 1.39, and 2.71 (s, 36H, atropoisomers), 7.62 (br s, 2H), 8.00, 8.06, and 8.11 (br s, 4H, atropoisomers), 8.05 and 8.12 (d, 1H, $J$ = 9 Hz, atropoisomers), 8.40 and 8.43 (d, 2H, $J$ = 9 Hz, atropoisomers), 8.57–8.59 (m, 6H), 8.78 (t, 2H, $J$ = 9 Hz), 8.80–8.81 (m, 4H), 8.92–8.94 (m, 2H), 8.97–9.11 (m, 10H), 9.78 and 9.80 (s, 2H, atropoisomers). $^{13}$C NMR (5% pyridine-$d_5$ in $CDCl_3$, 150 MHz): 29.6, 31.6, 34.8, 118.1, 120.4, 121.8, 122.35, 122.37, 122.5, 122.7, 122.72, 122.8, 123.6, 125.88, 125.95, 126.14, 126.16, 126.2, 126.29, 126.34, 126, 41, 126.47, 126.9, 127.1, 127.2, 127.3, 128.24, 128.26, 128.9, 129.0, 129.4, 129.7, 129.8, 131.6, 132.3, 132.6, 135.8, 139.6, 140.3, 142.2, 148.0, 148.1, 149.8, 150.6, 151.1. UV/vis ($CH_2Cl_2$) $\lambda$, nm, ($\varepsilon$): 304 (239778), 342 (45247), 427 (472969), 434 (359453), 513 (6346), 551 (30874), 588 (7212). HRMS: 1344.5046 ($M^+$ and $MH^+$), calcd. 1344.5043 for $C_{96}H_{72}N_4Zn$.

*[10,20-Bis-(3,5-di-tert-butylphenyl)-5,15-bis-(1-pyrenyl)porphyrin* ***2-H***. Porphyrin **2** (950 mg, 0.826 mmol) was dissolved in dichloromethane (100 mL). Concentrated hydrochloric acid (3 mL) was added and the resulting green solution was vigorously stirred for 30 s. The reaction mixture was quenched with pyridine, passed though plug of silica gel washing with dichloromethane. All purple fractions were collected, solvents were evaporated and the residue was crystallized from dichloromethane by adding methanol. Yield 850 mg (0.782 mmol, 95%). $^1$H NMR ($CDCl_3$, 400 MHz): 1.47, 1.48, and 1.49 (s, 36H, atropoisomers), 7.52 (t, 2H, $J$ = 9 Hz), 7.73–7.75 (m, 4H), 8.05–8.14 (m, 8H), 8.31–8.36 (m, 4H), 8.41 (d, 2H, $J$ = 8 Hz), 8.52–8.55 (m, 6H), 8.83 (d, 4H, $J$ = 4.8 Hz), 8.86 (t, 2H, $J$ = 8 Hz). $^{13}$C NMR ($CDCl_3$, 75 MHz): 31.7, 35.0, 117.8, 121.0, 121.8, 122.8, 124.1, 124.6, 125.3, 125.6, 126.3, 127.3, 127.6, 127.7, 128.0, 129.7, 129.9, 130.0, 130.8, 131.4, 131.8, 132.57, 132.63, 133.46, 133.51, 137.3, 140.9, 148.8. MALDI TOF: 1086.0 ($M^+$), requires 1086.6 for $C_{80}H_{70}N_4$.

*[10,20-Bis-(3,5-di-tert-butylphenyl)-5,15-bis-(1-pyrenyl)-porphyrinato(2-)]copper(II)* ***2-Cu***. To a solution of porphyrin **2-H** (100 mg, 0.092 mmol) in dichloromethane (100 mL), solution of $Cu(OAc)_2$*$2H_2O$ in methanol (10 mL) was added and the resulting mixture was refluxed for 1 h. The residue after evaporation of solvents was passed though a short plug of alumina washing with dichloromethane. Dichloromethane was evaporated in vacuum and the residue crystallized from dichloromethane by adding methanol. Yield 90 mg (0.078 mmol, 85%).$^1$H NMR ($CDCl_3$, 400 MHz): 1.38 (br s, 36H), 7.61, 8.03, 8.16, 8.28 (br s, 32H) broad signals due to the presence of copper(II) in the structure. $^{13}$C NMR ($CDCl_3$, 75 MHz): 31.6, 34.7, 120.5, 122.5, 123.4, 124.4, 125.1, 125.3, 126.3, 127.4, 127.6, 127.8, 130.8, 131.0, 131.7, 133.3, 148.3. UV/vis ($CH_2Cl_2$) $\lambda$, nm, ($\varepsilon$): 275 (74683), 337 (54521), 423 (409921), 541 (29288), 575 (5576). HRMS: 1147.4761 ($M^+$), calcd. 1147.4734 for $C_{80}H_{68}N_4Cu$.

*[10,20-Bis-(3,5-di-tert-butylphenyl)-5,15-bis-(1-pyrenyl)-porphyrinato(2-)]magnesium(II)* ***2-Mg***. A mixture of porphyrin **2-H** (100 mg, 0.092 mmol) and $MgI_2$ (100 mg) in pyridine (10 mL) was refluxed for 1 h. Reaction mixture was diluted with dichloromethane and passed though a short plug of alumina washing with dichloromethane. Dichloromethane was evaporated in vacuum and the residue crystallized from dichloromethane by adding methanol. Yield 95 mg (0.086 mmol, 93%). $^1$H NMR ($CDCl_3$, 400 MHz): 1.47, 1.48, and 1.49 (s, 36H), 7.47 (d, 1H, $J$ = 9 Hz), 7.49 (d, 1H, $J$ = 9 Hz), 7.68 (d, 2H, $J$ = 9 Hz), 7.71 (s, 2H), 8.03–8.13 (m, 8H), 8.30–8.33 (m, 4H), 8.41 (d, 2H, $J$ = 9 Hz), 8.50 (d, 2H, $J$ = 8 Hz), 8.53 (d, 4H, $J$ = 4.5 Hz), 8.84 (d, 4H, $J$ = 4.5 Hz), 8.88 (t, 2H, $J$ = 8 Hz). $^{13}$C NMR ($CDCl_3$, 75 MHz): 31.7, 35.0, 119.2, 120.4, 122.5, 123.3, 124.1, 124.7, 125.0, 125.3, 126.1, 127.1, 127.7, 127.8, 129.9, 130.0, 130.1, 131.1, 131.8, 132.5, 132.7, 132.8, 133.4, 133.5, 139.0, 142.4, 148.1, 148.2, 150.3, 150.7. UV/vis ($CH_2Cl_2$) $\lambda$, nm, ($\varepsilon$): 275 (67301), 338 (55958), 433 (468074), 525 (5750), 566 (22856), 606 (13367). HRMS: 1108.5298 ($M^+$), calcd. 1108.5289 for $C_{80}H_{68}N_4Mg$.

*[10,20-Bis-(3,5-di-tert-butylphenyl)-5,15-bis-(1-pyrenyl)-porphyrinato(2-)]lead(II)* ***2-Pb***. A mixture of porphyrin **2-H** (100 mg, 0.092 mmol) and $Pb(OAc)_2$*$3H_2O$ (100 mg) in pyridine (5 mL) was refluxed for 1 h. Reaction mixture was diluted with dichloromethane and passed though a short plug of alumina washing with dichloromethane. Dichloromethane was evaporated in vacuum and the residue crystallized from dichloromethane by adding methanol. Yield 95 mg (0.073 mmol, 80%). $^1$H NMR ($CDCl_3$, 500 MHz): 1.44–1.51 (m, 36H), 7.08 and 7.20 (d, 1H, J = 8 Hz), 7.05–7.61 (m, 2H), 7.73–7.75 (m, 2H), 7.87–8.68 (m, 22H), 8.82–9.07 (m, 5H). $^{13}$C NMR ($CDCl_3$, 75 MHz): 31.7, 31.8, 35.0, 117.8, 119.8, 119.83, 119.85, 120.8, 121.0, 121.8, 122.5, 122.7, 122.8, 124.0, 124.1, 124.6, 124.8, 125.2, 125.24, 125.29, 125.4, 125.5, 126.21, 126.25, 127.3, 127.4, 127.5, 127.55, 127.64, 127.7, 127.8, 127.9, 128.0, 129.3, 129.4, 129.5, 129.7, 129.9, 130.0, 130.3, 130.4, 130.6, 130.8, 130.9, 131.2, 131.3, 131.4, 131.7, 131.8, 131.96, 131.98, 132.1, 132.6, 132.7, 132.75, 133.5, 133.6, 133.8, 133.9, 137.3, 138.1, 138.2, 140.9, 141.8, 148.3, 148.5, 148.7, 149.6, 149.62, 149.66, 149.9, 150.0, 150.1, 150.2. UV/vis ($CH_2Cl_2$) $\lambda$, nm, ($\varepsilon$): 276 (80104), 340 (81161), 426 (90864), 472 (236200), 556 (5565), 612 (9467), 662 (16969). HRMS: 1292.5243 ($M^+$), calcd. 1292.5205 for $C_{80}H_{68}N_4Pb$.

*[10,20-Bis-(3,5-di-tert-butylphenyl)-5,15-bis-(1-pyrenyl)-porphyrinato(2-)](II)palladium* ***2-Pd***. A mixture of porphyrin **2-H** (100 mg, 0.092 mmol) and $PdCl_2$ (50 mg) in benzonitrile (25 mL) was refluxed for 3 h. Benzonitrile was distilled off in vacuum and the residue passed though a short plug of alumina washing with dichloromethane. Dichloromethane was evaporated in vacuum and the residue crystallized from dichloromethane by adding methanol. Yield 70 mg (0.059 mmol, 64%). $^1$H NMR ($CDCl_3$, 500 MHz): 1.45, 1.456, 1.46, and 1.54 (s, 36H, atropoisomers), 7.41–7.48 (m, 2H), 7.72–7.75 (m, 4H), 8.05 (d, 4H, $J$ = 2 Hz), 8.07 (d, 2H, $J$ = 8 Hz), 8.10 (d, 2H, $J$ = 8 Hz), 8.31–8.35 (m, 4H), 8.40 (d, 2H, J = 8 Hz), 8.48–8.53 (m, 6H), 8.78 (d, 4H, $J$ = 4.5 Hz), 8.78–8.80 (m, 2H). $^{13}$C NMR ($CDCl_3$, 75 MHz): 31.7, 35.0, 119.5, 121.0, 122.8, 123.4, 124.1, 124.6, 125.3, 125.5, 126.3, 127.2, 127.6, 127.7, 128.0, 129.4, 130.8, 130.9, 131.4, 131.6, 131.7, 132.2, 132.3, 133.2, 136.7, 140.6, 141.9, 142.3, 148.7. UV/vis ($CH_2Cl_2$) $\lambda$, nm, ($\varepsilon$): 275 (71971), 338 (49029), 424 (323602), 526 (36618), 557 (6234). HRMS: 1190.4529 ($M^+$ and $MH^+$), calcd. 1190.4473 for $C_{80}H_{68}N_4Pd$.

*[10,20-Bis-(3,5-di-tert-butylphenyl)-5,15-bis-(1-pyrenyl)-porphyrinato(2-)](II)platinum* ***2-Pt***. A mixture of porphyrin **2-H** (100 mg, 0.092 mmol) and $PtCl_2$ (50 mg) in benzonitrile (25 mL) was refluxed for 3 h. Benzonitrile was distilled off in vacuum and the residue passed though a short plug of alumina washing with dichloromethane. Dichloromethane was evaporated in vacuum and the residue crystallized from dichloromethane by adding methanol. Yield 80 mg (0.063 mmol, 68%). $^1$H NMR ($CDCl_3$, 400 MHz): 1.446, 1.45, 1.46, and 1.53 (s, 36H, atropoisomers), 7.44 and 7.50 (d, 2H, $J$ = 9 Hz, atropoisomers), 7.72 (t, 2H, $J$ = 2 Hz), 7.73 and 7.76 (d, 2H, $J$ = 10 Hz, atropoisomers), 7.97–8.08 (m, 6H), 8.12 (d, 2H, $J$ = 8 Hz), 8.32 (t, 4H, $J$ = 10 Hz), 8.39 (d, 2H, $J$ = 9 Hz), 8.43 and 8.44 (d, 4H, $J$ = 5 Hz, atropoisomers), 8.52 and 8.54 (d, 2H, $J$ = 8 Hz, atropoisomers), 8.73 (d, 4H, $J$ = 5 Hz), 8.78 and 8.81 (d, 2H, $J$ = 8 Hz, atropoisomers). $^{13}$C NMR ($CDCl_3$, 125 MHz): 31.7, 35.0, 120.1, 121.1, 122.9, 123.9, 124.2, 124.6, 125.3, 126.3, 127.0, 127.7, 127.72, 128.0, 129.0, 129.1, 129.2, 130.6, 130.9, 131.4, 131.5, 131.7, 132.0, 132.1, 133.1, 133.12, 136.24, 136.26, 140.2, 141.2, 141.6, 148.82, 148.8, 148.9. UV/vis ($CH_2Cl_2$) $\lambda$, nm, ($\varepsilon$): 275 (87028), 339 (57026), 410 (297768), 513 (43155), 542 (10805). HRMS: 1279.5071 ($M^+$ and $MH^+$), calcd. 1279.5086 for $C_{80}H_{68}N_4Pt$.

*[10,20-Bis-(3,5-di-tert-butylphenyl)-5,7,15,17-bis-(1,8-naphthyl)-porphyrinato(2-)]zinc(II) and [10,20-bis-(3,5-di-tert-butylphenyl)-3,5,15,17-bis-(1,8-naphthyl)-porphyrinato(2-)]zinc(II)* ***1d.*** *Bis*-naphthyl-porphyrin **1***MeOH (0.97 g, 0.937 mmol) in a glass boat was placed into a glass tube. The tube was purged with nitrogen and kept under positive nitrogen atmosphere. The tube was placed into furnace preheated to 530 °C and kept there for 12 min under nitrogen atmosphere. First, the furnace temperature rose to 530 °C in 1−2 min and after additional ca. 2 min starting material melted. Reaction mixture turned brown after 3−4 min and bubbles appeared. After ca. 5 min the tube was taken out from the furnace and cooled to room temperature under nitrogen. Prolonged heating causes reduced yields of the doubly fused product **1d**. The crude mixture was dissolved in dichloromethane (100 mL) and separated on alumina column (400 g). Elution with hexanes:dichloromethane:pyridine = 700:300:5 mixture gave crude doubly fused porphyrin **1d** which was recrystallized from dichloromethane by layered addition of methanol to give **1d** (70 mg, 0.07 mmol, 7%). $^1$H NMR contained only broad signals due to pronounced aggregation or forming oxidized paramagnetic species. UV/vis ($CH_2Cl_2$) $\lambda$, nm, ($\varepsilon$): 418 (70111), 486 (147059), 648 (25731), 730 (39704). HRMS: 996.4106 ($M^+$ and $MH^+$), calcd. 996.4104 for $C_{68}H_{60}N_4Zn$. The second fraction (dichloromethane−pyridine = 1000:5) contained doubly fused product with the loss of one di-*tert*-butylphenyl group (100 mg, 13%): MALDI-TOF: 807.27 ($M^+$), calcd. 808.25 for $C_{54}H_{40}N_4Zn$.

*[10,20-Bis-(3,5-di-tert-butylphenyl)-3,5-(1,10-pyrenyl)-15-(1-pyrenyl)porphyrinato(2-)]zinc(II)* ***(2m)*** *and [10,20-bis-(3,5-di-tert-butylphenyl)-3,5,13,15-bis-(1,10-pyrenyl)-porphyrinato(2-)]zinc(II)* ***(2d).*** The above *bis*-pyrenyl-porphyrin **2***MeOH (1 g, 0.845 mmol) in a glass boat was placed into a glass tube. The tube was purged with nitrogen and kept under positive nitrogen atmosphere. The tube was placed into furnace preheated to 530 °C and kept there for 5 min under nitrogen atmosphere. First, the furnace temperature rose to 530 °C in 1−2 min and after additional ca. 1−2 min starting material melted. Reaction mixture turned brown immediately and bubbles appeared. After ca. 0.5 min the tube was taken out from the furnace and cooled to room temperature under nitrogen. Prolonged heating causes reduced yields of the doubly fused product **2d**. This cycle was repeated 5 times (totally, 6 g of porphyrin **2**). The crude mixture was dissolved in dichloromethane (100 mL) with addition of hexanes (300 mL) and pyridine (5 mL) and separated on alumina column (400 g). Elution with dichloromethane gave first fraction which contained compound **2m**. Elution with hexanes:dichloromethane:pyridine = 700:300:5 mixture gave crude doubly fused porphyrin **2d** which was recrystallized from dichloromethane by layered addition of methanol to give **2d** (ca. 93−95% purity 1.80 g, 30%). Elution with dichloromethane:pyridine = 1000:5 mixture gave a mixture of doubly fused porphyrins with the loss of one di-*tert*-butyl-phenyl group which were recrystallized from dichloromethane-pyridine by layered addition of methanol (2.3 g, 38%). Higher purity doubly fused porphyrin **2d** can be obtained by column chromatography on silica gel (gradient elution with hexanes:dichloromethane mixtures 1000:50 to 800:200).

First fraction containing compound **2m** was additionally purified by silica gel column (gradient elution with hexanes:ethyl acetate mixtures 1000:5 to 1000:15) and crystallized from dichloromethane by layered addition of methanol to give compound **2m** (0.54 g, 9%).

*[10,20-Bis-(3,5-di-tert-butylphenyl)-5,7-bis-(1,10-pyrenyl)-15-(1-pyrenyl)porphyrinato(2-)]zinc(II)* ***2m.*** $^1$H NMR (5%-pyridine-$d_5$ in $C_6D_6$, 500 MHz): 1.49, 1.507, 1510, and 1.52 (s, 36H, atropoisomers), 7.39 (d, 1H, $J$ = 9.5 Hz), 7.59 (d, 1H, $J$ = 9.5 Hz), 7.78−7.85 (m, 3H), 7.94−7.96 (m, 2H), 8.01 (s, 1H), 8.02−8.09 (m, 5H), 8.14 (d, 1H, $J$ = 9.5 Hz), 8.24 (d, 1H, $J$ = 8 Hz), 8.32 (d, 1H, $J$ = 8 Hz), 8.39 (t, 1H, $J$ = 1.5 Hz), 8.45 (t, 1H, $J$ = 1.5 Hz), 8.53 (t, 1H, $J$ = 1.5 Hz), 8.55 (d, 1H, $J$ = 4.5 Hz), 8.56 (t, 1H, $J$ = 1.5 Hz), 8.63 (d, 1H, $J$ = 4.5 Hz), 8.84 (d, 1H, $J$ = 8 Hz), 9.03 (d, 1H, $J$ = 4.5 Hz), 9.09 (d, 1H, $J$ = 4.5 Hz), 9.13 (s, 1H), 9.22 (d, 1H, $J$ = 4.5 Hz), 9.48 (d, 1H, $J$ = 8.5 Hz), 9.53 (d, 1H, $J$ = 4.5 Hz), 9.98 (s, 1H). $^{13}$C NMR (5%-pyridine-$d_5$ in $C_6D_6$, 125 MHz): 30.2, 31.85, 31.86, 31.89, 35.18, 35.20, 114.3, 119.0, 121.00, 121.03, 124.3, 124.6, 124.8, 124.9, 125.0, 125.3, 125.4, 125.7, 125.8, 126.3, 126.4, 126.8, 127.4, 127.7, 129.1, 130.7, 130.86, 130.90, 131.0, 131.2, 131.4, 131.6, 131.8, 131.9, 132.2, 132.3, 132.5, 132.69, 132.75, 132.8, 132.9, 133.0, 133.8, 133.9, 137.4, 138.0, 139.0, 143.4, 143.5, 146.8, 149.08, 149.10, 149.23, 149.26, 150.3, 150.5, 150.6, 151.0, 151.8, 152.0, 152.3. UV/vis ($CH_2Cl_2$) $\lambda$, nm, ($\varepsilon$): 706 (43480), 495 (206480), 386 (40296), 339 (45680), 324 (38374), 275 (51790), 264 (44275). Emission ($CH_2Cl_2$): $\lambda_{max}$, 722 nm; quantum yield, 8.0%. HRMS: 1146.4581 ($M^+$), calcd. 1146.4573 for $C_{80}H_{66}N_4Zn$. Elemental analysis for $C_{80}H_{66}N_4Zn$*MeOH: calcd C 82.39, H 5.97, N 4.74; found C 82.69, H 5.91, N 4.86.

*[10,20-Bis-(3,5-di-tert-butylphenyl)-5,7,15,17-bis-(1,10-pyrenyl)-porphyrinato(2-)]zinc(II) and [10,20-bis-(3,5-di-tert-butylphenyl)-3,5,15,17-bis-(1,10-pyrenyl)-porphyrinato(2-)]zinc(II)* ***2d.*** (1:1 mixture of *anti/syn* regioisomers). $^1$H NMR (5%-pyridine-$d_5$ in $C_6D_6$, 25 °C, 500 MHz, two regioisomers): 1.53, 1.59, and 1.61 (s, 36H, regioisomers), 7.81 and 7.82 (d, 2H, $J$ = 8 Hz, regioisomers), 7.91−8.03 (m, 8H), 8.1 and 8.17 (t, 2H, $J$ = 1.5 Hz, regioisomers), 8.26 and 8.28 (d, 2H, $J$ = 8.5 Hz, regioisomers), 8.40, 8.55, and 8.62 (d, 4H, $J$ = 1.5 Hz, regioisomers), 9.00 and 9.08 (d, 2H, $J$ = 4.5 Hz, regioisomers), 9.07 and 9.12 (s, 2H, regioisomers), 9.28 and 9.36 (d, 2H, $J$ = 4.5 Hz, regioisomers), 9.33 and 9.35 (d, 2H, $J$ = 8 Hz, regioisomers), 9.78 and 9.84 (s, 2H, regioisomers). $^1$H NMR (5%-pyridine-$d_5$ in $C_6D_6$, 75 °C, 500 MHz, two regioisomers): 1.51, 1.57, and 1.60 (s, 36H regioisomers), 7.08 (t, 2H, $J$ = 8 Hz), 7.92 (t, 2H, $J$ = 9 Hz), 7.99 (d, 4H, $J$ = 8 Hz), 8.04 (s, 2H), 8.06 and 8.15 (s, 2H, regioisomers), 8.02−8.06 (m, 4H), 8.45 and 8.54 (d, 2H, $J$ = 1 Hz, regioisomers), 8.90 and 8.93 (d, 2H, $J$ = 4.5 Hz, regioisomers), 9.11 and 9.13 (s, 2H, regioisomers), 9.23−9.30 (m, 4H), 9.67 and 9.70 (s, 2H, regioisomers). $^{13}$C NMR (5%-pyridine-$d_5$ in $C_6D_6$, 25 °C, 125 MHz, two regioisomers): 30.1, 31.84, 31.92, 31.94, 35.20, 114.0, 114.2, 121.1, 121.3, 121.4, 122.7, 124.1, 124.2, 124.8, 125.4, 125.41, 125.8, 126.4, 126.9, 127.4, 127.42, 127.5, 128.9, 129.0, 130.3, 130.5, 130.7, 130.8, 131.8, 132.0, 132.9, 133.0, 133.03, 133.3, 133.4, 133.6, 136.5, 136.6, 138.0, 138.4, 143.3, 143.4, 146.7, 147.4, 149.2, 150.1, 150.4, 150.5, 150.8, 151.1. Emission ($CH_2Cl_2$): $\lambda_{max}$, 815 nm; quantum yield, 10%. MALDI TOF: 1143.9 ($M^+$), requires 1144.44 for $C_{80}H_{64}N_4Zn$. HRMS: 1144.4410 ($M^+$), calcd. 1144.4417 for $C_{80}H_{64}N_4Zn$. Elemental analysis for $C_{80}H_{64}N_4Zn$*MeOH: calcd C 82.53, H 5.81, N 4.75; found C 82.92, H 5.77, N 4.78.

*anti-[10,20-Bis-(3,5-di-tert-butylphenyl)-5,7,15,17-bis-(1,10-pyrenyl)-porphyrinato(2-)]zinc(II)* ***anti-2d.*** ***anti*-2d** can be obtained by separation of a mixture of *anti/syn* **2d** using silica gel column (gradient elution with benzene:hexanes −1:5 to 2:3) by collecting first fraction followed by layered crystallization from dichloromethane:methanol mixture. $R_f$ = 0.42 (hexanes−benzene = 1:1). $^1$H NMR (5%-pyridine-$d_5$ in $C_6D_6$, 25 °C, 500 MHz): 1.59 (s, 36H, *t*-Bu), 7.83 (t, 2H, $J$ = 8 Hz, $H^7{}_{pyrene}$), 7.93 (d, 2H, $J$ = 9 Hz, $H_{pyrene}$), 7.99 (d, 2H, $J$ = 9 Hz, $H_{pyrene}$), 8.00 (d, 2H, $J$ = 8 Hz, $H^6{}_{pyrene}$), 8.05 (d, 2H, $J$ = 8 Hz, $H^8{}_{pyrene}$), 8.04 (t, 2H, $J$ = 1.5 Hz, *p-H of Ar*), 8.27 (d, 2H, $J$ = 9 Hz, $H_{pyrene}$), 8.50−8.51 (m, 2H, *o-H* of Ar), 8.55 (d, 2H, $J$ = 1.5 Hz, *o-H* of Ar), 9.00 (d, 2H, $J$ = 4.5 Hz, *β*-pyrrolic $H^{7,17}{}_{porph}$), 9.13 (s, 2H, *β*-pyrrolic $H^{2,12}{}_{porph}$), 9.27 (d, 2H, $J$ = 4.5 Hz, *β*-pyrrolic $H^{8,18}{}_{porph}$), 9.33 (d, 2H, $J$ = 8 Hz, $H_{pyrene}$), 9.84 (s, 2H, $H^9{}_{pyrene}$).$^{13}$C NMR (5%-pyridine-$d_5$ in $C_6D_6$, 125 MHz): 32.0, 35.3, 114.3, 121.3, 122.9, 124.4, 124.5, 125.4, 125.9, 126.4, 126.75, 126.81, 127.4, 129.2, 130.5, 130.8, 131.8, 132.0, 133.0, 133.3, 133.5, 136.7, 138.1, 143.4, 146.8, 149.5, 150.2, 150.4, 151.2. UV/vis ($CH_2Cl_2$) $\lambda$, nm, ($\varepsilon$): 815 (81206), 741 (20628), 656 (5045), 559 (54452), 504 (151197). Emission ($CH_2Cl_2$): $\lambda_{max}$, 839 nm; quantum yield, 7.7%.

*syn-[10,20-Bis-(3,5-di-tert-butylphenyl)-3,5,15,17-bis-(1,10-pyrenyl)-porphyrinato(2-)]zinc(II)* ***syn-2d.*** ***syn*-2d** can be obtained by separation of a mixture of *anti/syn* **2d** using silica gel column (gradient elution with benzene−hexanes= −1:5 to 2:3) by collecting the last fractions followed by layered crystallization from dichloromethane-methanol mixture. $R_f$ = 0.31 (hexanes−benzene = 1:1). $^1$H NMR (5%-pyridine-$d_5$ in $C_6D_6$, 25 °C, 500 MHz): 1.53 (s, 18H, *t*-Bu), 1.61 (s, 18H, *t-Bu*), 7.82 (t, 2H, $J$ = 8 Hz, $H^7{}_{pyrene}$), 7.93 (d, 2H, $J$ = 9 Hz, $H_{pyrene}$), 7.99 (d, 2H, $J$ = 9 Hz, $H_{pyrene}$), 8.00 (t, 1H, $J$ = 1.5 Hz, *p-H* of Ar), 8.00 (d, 2H, $J$ = 8 Hz, $H^6{}_{pyrene}$), 8.05 (d, 2H, $J$ = 8 Hz, $H^8{}_{pyrene}$), 8.17 (t, 1H, $J$ = 1.5 Hz, *p-H* of Ar), 8.27 (d, 2H, $J$ = 9 Hz, $H_{pyrene}$), 8.40 (2, 2H, $J$ = 1.5 Hz, *o-H* of Ar), 8.61 (d, 2H, $J$ = 1.5 Hz,


dx.doi.org/10.1021/jo201490y | *J. Org. Chem.* 2012, 77, 143−159

*o-H* of Ar), 9.07 (d, 2H, $J$ = 4.5 Hz, $\beta$-pyrrolic $H^{7,17}{}_{porph}$), 9.08 (s, 2H, $\beta$-pyrrolic $H^{2,12}{}_{porph}$), 9.36 (d, 2H, $J$ = 4.5 Hz, $\beta$-pyrrolic $H^{8,18}{}_{porph}$), 9.37 (d, 2H, $J$ = 8 Hz, $H_{pyrene}$), 9.78 (s, 2H, $H^{9}{}_{pyrene}$).$^{13}$C NMR (5%-pyridine-$d_5$ in $C_6D_6$, 125 MHz): 30.2, 31.9, 32.0, 114.0, 121.1, 121.4, 122.52, 122.54, 123.3, 123.34, 124.3, 125.0, 125.5, 125.9, 126.3, 126.8, 127.4, 127.5, 128.6, 128.7, 128.8, 129.0, 129.7, 129.85, 129.9, 130.5, 130.80, 130.85, 131.8, 131.9, 132.9, 133.0, 133.7, 136.6, 138.5, 143.3, 143.5, 147.4, 149.2, 149.5, 150.6, 150.8. UV/vis ($CH_2Cl_2$) $\lambda$, nm, ($\varepsilon$): 811 (91461), 736 (26446), 657 (10865), 527 (145812). Emission ($CH_2Cl_2$): $\lambda_{max}$, 829 nm; quantum yield, 12.8%.

*anti-[10-(3,5-Di-tert-butylphenyl)-5,7,15,17-bis-(1,10-pyrenyl)-porphyrinato(2-)]zinc(II), syn-[10-(3,5-di-tert-butylphenyl)-3,5,15,17-bis-(1,10-pyrenyl)-porphyrinato(2-)]zinc(II) and syn-[20-(3,5-di-tert-butylphenyl)-3,5,15,17-bis-(1,10-pyrenyl)-porphyrinato(2-)]zinc(II).* Compounds ***anti*-2d** and ***syn*-2d** with the loss of one di-*tert*-butylphenyl group can be obtained as a mixture of isomers by chromatography separation on alumina (fractions eluting with dichloromethane−pyridine = 1000:5). $^1$H NMR (5%-pyridine-$d_5$ in $C_6D_6$, 25 °C, 500 MHz, broad signals, isomers): 1.51−1.65 (m, 18H, *t*-Bu), 7.61−8.70 (m, 17H), 9.02−9.60 (m, 9H), 9.78 and 9.94 (s, 2H, isomers). UV/vis ($CH_2Cl_2$) $\lambda$, nm: 806, 729, 553sh, 520sh, 501, 369, 345. HRMS: 956.2823 ($M^+$), requires 956.2852 for $C_{66}H_{44}N_4Zn$.

*[10,20-Bis-(3,5-di-tert-butylphenyl)-5,7,15,17-bis-(1,12-perylenyl)-porphyrinato(2-)]zinc(II) and [10,20-bis-(3,5-di-tert-butylphenyl)-3,5,15,17-bis-(1,12-perylenyl)-porphyrinato(2-)]zinc(II)* ***3d***. *Bis*-perylenyl porphyrin **3** (380 mg, 0.304 mmol) was dissolved in dry dichloromethane (600 mL) under nitrogen atmosphere at 20 °C and to the resulting solution anhydrous $FeCl_3$ (1.2 g) was added at once. The reaction mixture was vigorously stirred for 15 min and after that quenched with pyridine (5 mL). The resulting purple solution was passed through short plugs of alumina (prewashed with dichloromethane−pyridine = 1000:5) and silica gel (prewashed with dichloromethane-pyridine =1000:5) eluting with dichloromethane−pyridine = 1000:5. All purple fractions were collected. MALDI-TOF indicated the presence of the corresponding free-base porphyrin fused with two perylene rings: 1182.43 ($M^+$), calcd. 1182.56 for $C_{88}H_{70}N_4$. Solution of $Zn(OAc)_2$*$2H_2O$ (1 g) in methanol (30 mL) was added and stirred at room temperature for 2 h. After that solvents were evaporated in vacuum and the residue passes through short plug of silica gel (prewashed with dichloromethane−pyridine = 1000:5) eluting with dichloromethane−pyridine = 1000:5. Solvents were evaporated in vacuum and the residue was crystallized from dichloromethane by layered addition of methanol. Yield of **3d** 250 mg (0.200 mmol, 67%). Fused product **3d** can be also obtained by thermal cyclodehydrogenation method at 550 °C as evidenced by absorption peaks corresponding to the doubly fused product at 900 nm in the crude reaction mixture and peaks of the molecular ion in MALDI-TOF spectrum. $^1$H NMR (5% pyridine-$d_5$ in $C_6D_6$, 500 MHz, *syn*/*anti* = 0.75:1): 1.54 (*syn*), 1.60 (*anti*) and 1.62 (*syn*) (s, 36H, *t*-Bu), 7.55 (*anti*) and 7.56 (*syn*) (d, 4H, $J$ = 8 Hz, $H_{perylene}$), 8.00 (*syn*), 8.09 (*anti*) and 8.14 (*syn*) (t, 2H, $J$ = 1.5 Hz, *o-H* of Ar), 8.15−8.19 (m, 4H), 8.26 (*syn*) and 8.32 (*anti*) (d, 2H, $J$ = 8 Hz, $H_{perylene}$), 8.37−8.52 (m, 8H), 8.43 (*syn*), 8.55 (*anti*) and 8.58 (*syn*) (d, 4H, $J$ = 1.5 Hz, *p-H* of Ar), 8.72 (*anti*) and 8.77 (*syn*) (d, 2H, $J$ = 8 Hz, $H_{perylene}$), 9.02 (*anti*) and 9.11 (*syn*) (d, 2H, $J$ = 4.5 Hz, $\beta$-pyrrolic $H_{porph}$), 9.09 (*anti*) and 9.21 (*syn*) (d, 2H, $J$ = 4.5 Hz, $\beta$-pyrrolic $H_{porph}$), 9.59 (*syn*) and 9.66 (*anti*) (s, 2H, $H^{12}{}_{perylene}$). $^{13}$C NMR (5%-pyridine-$d_5$ in $C_6D_6$, 125 MHz): 30.2, 31.9 (*syn*), 31.95 (*anti*) and 31.99 (*syn*), 113.1 (*syn*) and 113.4 (*anti*), 121.2, 121.56 (*anti*) and 121.59 (*syn*), 121.7, 121.8, 121.86, 121.92, 122.0, 122.05, 122.15, 122.3, 123.5, 125.4 (*anti*) and 125.5 (*syn*), 125.55 (*anti*) and 125.6 (*syn*), 126.0, 126.1, 126.3, 127.1, 127.4, 128.48, 128.52, 129.13, 129.17, 129.4, 129.89, 129.90, 130.48 (*syn*) and 130.52 (*anti*), 131.36 (*syn*) and 131.40 (*anti*), 131.66, 131.72, 131.9, 132.7 (*syn*) and 132.9 (*anti*), 133.2 (*anti*) and 133.5 (*syn*), 134.98 (*anti*) and 135.00 (*syn*), 135.2, 137.6, 138.4, 139.61 (*syn*) and 139.71 (*anti*), 143.42, 143.43, 143.46, 143.2 (*anti*) and 146.8 (*syn*), 148.9 (*syn*) and 149.2 (*anti*), 149.52 (*anti*) and 149.64 (*syn*), 150.2, 150.3, 150.8, 151.4 (*syn*) and 151.6 (*anti*). UV/vis ($CH_2Cl_2$) $\lambda$, nm, ($\varepsilon$): 297 (18355), 426 (20215), 469 (21794), 538 (71476), 592 (44671), 901 (65502). HRMS: 1244.4745 ($M^+$ and $MH^+$), calcd. 1244.4730 for $C_{88}H_{68}N_4Zn$.

*[10,20-Bis-(3,5-di-tert-butylphenyl)-5,7,15,17-bis-(1,12-coronenyl)-porphyrinato(2-)]zinc(II) and [10,20-bis-(3,5-di-tert-butylphenyl)-3,5,15,17-bis-(1,12-coronenyl)-porphyrinato(2-)]zinc(II)* ***4d***. Bis-coronenyl-porphyrin **4** (90 mg, 0.067 mmol) in a glass boat was placed into a glass tube. The tube was purged with nitrogen and kept under positive nitrogen atmosphere. The tube was placed into furnace preheated to 560 °C and kept there for 5 min under nitrogen atmosphere. First, the furnace temperature rose to 560 °C in 1−2 min and after additional ca. 1−2 min starting material melted. Once porphyrin material melted, the tube was taken out from the furnace and cooled by liquid nitrogen. The crude mixture was dissolved in dichloromethane (100 mL) and pyridine (3 mL) and separated on alumina column (50 g). Elution with dichloromethane−pyridine = 1000:5 mixture gave doubly fused porphyrin **4d** which was recrystallized from dichloromethane by layered addition of methanol to give **4d** (12 mg, 0.009 mmol, 13%). $^1$H NMR spectra of porphyrin **4d** contain only broad signals using different solvents and temperatures due to aggregation in solution. Taking into account significant fragmentation of the product in mass spectra, the chromatographically pure material may have admixtures of the corresponding fused products with the loss of one or two di-*tert*-butyl groups. UV/vis ($CH_2Cl_2$) $\lambda$, nm, ($\varepsilon$): 437 (102102), 494 (220965), 687 (54277), 779 (81911). MALDI-TOF: 1340.14 ($M^+$), calcd. 1340.47 for $C_{96}H_{68}N_4Zn$; 1152.02 ($M^+$− 188 ($C_{14}H_{21}$ = di-*tert*-butylphenyl group+H)), calcd 1152.32 for $C_{82}H_{48}N_4Zn$; 964.34 ($M^+$− 376 ($C_{28}H_{42}$ = 2*di-*tert*-butylphenyl group +2H)), calcd 964.16 for $C_{68}H_{28}N_4Zn$.

*[5,15-Bis-(1-pyrenyl)porphyrinato(2-)]zinc(II).* Trifluoroacetic acid (2 mL) was added to a stirred solution of 1-pyrenecarboxaldehyde (3.7 g, 15.92 mmol) and dipyrromethane (2.34 g, 15.92 mmol) under nitrogen in dichloromethane (2 L). The reaction mixture was stirred at ambient temperature in dark for 48 h. After that DDQ (5.36 g) was added and stirring continued for an additional hour. The reaction mixture was quenched with triethylamine (10 mL) and passed through filter filled with silica gel (50 g) washing with dichloromethane. All purple fractions were collected, dichloromethane evaporated and the residue passed through filter filled with alumina (50 g) washing with dichloromethane. All purple fractions were collected, dichloromethane was evaporated to a volume 500 mL. To this solution of the free-base *bis*-pyrenyl-porphyrin, 30 mL of saturated solution of zinc(II) acetate in methanol (10 mL) was added and the resulting mixture was stirred for 3 h at ambient temperature. The reaction mixture was washed with water and dichloromethane solution was passed through filter filled with silica gel (50 g) washing with dichloromethane. The residue after evaporation of solvent was crystallized from dichloromethane by adding methanol to give [5,15-*bis*-(1-pyrenyl)porphyrinato(2-)]zinc-(II) (430 mg, 0.56 mmol, 7%).

*[10,20-Bis-bromo-5,15-bis-(1-pyrenyl)porphyrinato(2-)]zinc(II).* NBS (194 mg, 1.09 mmol, 2.1 equiv.) was added to a stirred solution of the above 5,15-*bis*-(1-pyrenyl)porphyrinato(2-)]zinc(II) (402 mg, 0.519 mmol) in dichloromethane (300 mL) and pyridine (5 mL) at −10 °C (NaCl/ice bath) under nitrogen atmosphere. Reaction mixture was stirred at the same temperature for 10 min, then was allowed to warm to 0 °C in 5 min (water bath) and after that reaction mixture was quenched with acetone (20 mL). Crude reaction mixture was passed through silica gel column, eluting with dichloromethane−pyridine mixture (100:1). All green-purple fractions were collected, solvents were evaporated, the residue was dissolved in dichloromethane−pyridine mixture (95:5, 100 mL) and 200 mL of methanol was added to precipitate brominated porphyrin. All crystals were collected by filtration after 30 min to give [10,20-*bis*-bromo-5,15-*bis*-(1-pyrenyl)-porphyrinato(2-)]zinc(II) (435 mg, 0.47 mmol, 90%). $^1$H NMR (5% pyridine-$d_5$ in $CDCl_3$, 500 MHz, atropoisomers): 6.93 (t, 2H, $J$ = 8 Hz), 7.19 (d, 2H, $J$ = 10 Hz), 7.61 (d, 2H, $J$ = 10 Hz), 8.06−8.09 (m, 4H), 8.32−8.36 (m, 4H), 8.42 (d, 2H, $J$ = 8 Hz), 8.52 (d, 4H, $J$ = 4.5 Hz), 8.79 (d, 2H, $J$ = 8 Hz), 9.55 (d, 4H, $J$ = 4.5 Hz).

*[5,10,15,20-Tetrakis-(1-pyrenyl)porphyrinato(2-)]zinc(II)* ***5***.[26] A mixture of the above [10,20-*bis*-bromo-5,15-*bis*-(1-pyrenyl)-porphyrinato(2-)]zinc(II) (400 mg, 0.429 mmol), cesium carbonate


dx.doi.org/10.1021/jo201490y | J. Org. Chem. 2012, 77, 143−159

(1.45 g, 10 equiv.), $Pd(PPh_3)_4$ (50 mg, 10 mol %), pyridine (2 mL) and 4,4,5,5-tetramethyl-2-(pyren-1-yl)-1,3,2-dioxaborolane (310 mg, 0.95 mmol, 2.2 equiv.) in toluene (150 mL) was degassed and refluxed under nitrogen for 12 h. Reaction mixture was cooled and passed consecutively through pads of Celite, silica gel and neutral alumina washing with toluene. Toluene was distilled off in vacuum, the residue was separated by column chromatography on silica gel (gradient elution with hexanes−ethyl acetate 1000:10 to 800:200) to afford [5,10,15,20-tetrakis-(1-pyrenyl)porphyrinato(2-)]zinc(II)[26] **5** (260 mg, 0.22 mmol, 50%). $^1$H NMR (5% pyridine-$d_5$ in $CDCl_3$, 500 MHz, mixture of atropoisomers): 7.21−7.30 (m, 2H), 7.35 and 7.39 (d, 2H, $J$ = 10 Hz, atropoisomers), 7.45−7.63 (m, 6H), 7.91−8.00 (m, 8H), 8.18 and 8.27 (d, 8H, $J$ = 10 Hz, atropoisomers), 8.20−8.23 (m, 4H), 8.35−8.40 (m, 10H), 8.71−8.85 (m, 4H). $^1$H NMR (5% pyridine-$d_5$ in $CDCl_3$, 125 MHz): (118.56, 118.58, 118.61, 118.63 − atropoisomers); 122.3, 123.6, 124.5, 124.9, 125.2, 126.0; (127.01, 127.04, 127.09, 127.15 − atropoisomers); (127.25, 127.27, 127.33, 127.35 − atropoisomers); 127.5, 130.6, 130.9, 131.6, 131.88, 131.90, 131.93, 131.97, 132.01, 132.42, 132.46, 132.50, 132.54, 132.60, 133.10, 133.14, 133.20, 133.25, 133,28, 133.35, 138.2; (150.92, 150.94, 150.95, 150.97 − atropoisomers). UV/vis (5%-pyridine in $CH_2Cl_2$) $\lambda$, nm, ($\varepsilon$): 606 (12286), 566 (29395), 441 (461248), 337 (100582), 323 (93953). MALDI TOF: 1172.60 ($M^+$), requires 1172.29 for $C_{84}H_{44}N_4Zn$. HRMS: 1173.2915 ($MH^+$), calcd. 1173.2930 for $C_{84}H_{45}N_4Zn$.

*[3,5,8,10,13,15,18,20-Tetrakis-(1,10-pyrenyl)porphyrinato(2-)]-zinc(II)* ***5t***. (mixture of regioisomers). The above porphyrin **5***MeOH (50 mg, mmol) in a glass boat was placed into a glass tube. The tube was purged with nitrogen and kept under positive nitrogen atmosphere. The tube was placed into furnace preheated to 560 °C and kept there for 5 min under nitrogen atmosphere. First, the furnace temperature rose to 560 °C in 1−2 min and after additional ca. 1−2 min starting material melted. Reaction mixture turned dark and the bubbles appeared. After ca. 0.5 min the tube was taken out from the furnace and cooled to room temperature under nitrogen. The crude mixture was dissolved in dichloromethane (100 mL) with addition of pyridine (10 mL, sonication is required for dissolving crude reaction mixture) and separated on silica gel column (elution with dichloromethane−pyridine 1000:10 mixture). Compound **5t** was crystallized from dichloromethane-pyridine by layered addition of methanol. Yield: 15 mg, 30%. $^1$H NMR (dilute solution in 5%-pyridine-$d_5$ in $C_6D_6$, 75 °C, 600 MHz, signal assignment for possible regioisomers could not be done, longer acquisition time required, signal broadening due to aggregation): 7.63 (d, 4H, $J$ = 8 Hz), 7.74−7.84 (m, 12H), 7.88−7.97 (m, 16H), 8.03 (d, 4H, $J$ = 9 Hz). UV/vis (5% pyridine in $CH_2Cl_2$) $\lambda$, nm ($\varepsilon$): 1003 (13954), 873 (43861), 813 (30458), 620 (73072), 576 (70842). MALDI-TOF MS (without matrix): 1164.32 ($M^+$), requires 1164.22 for $C_{84}H_{36}N_4Zn$. Peak of the molecular ion could not be obtained by using ESI/APCI MS. $^{13}$C NMR (5% pyridine-$d_5$ in $C_6D_6$, 125 MHz, weak signals): 124.0, 125.07, 125.10, 125.17, 126.10, 126.15, 126.8, 127.4, 127.5, 128.9, 129.6, 129.9, 131.6.

*Thermal Fusion of Metalated Pyrenyl-porphyrins* ***2-M***. The corresponding porphyrin **2-M** in a glass boat was placed into a glass tube. The tube was purged with nitrogen and kept under positive nitrogen atmosphere. The tube was placed in a furnace preheated to 530 °C (M = Mg, Cu, Pb) or 560 °C (M = Pt, Pd,) and kept there for 4−10 min. Starting material melts, turns brown with appearance of bubbles. After additional ca. 0.5 min after melting of the material the tube was taken out from the furnace and cooled to room temperature under nitrogen. UV−vis near IR absorption spectra (see main text, Figure 6e) of crude reaction mixtures demonstrate nearly quantitative conversion of starting porphyrinic material into doubly fused products. Mass spectra of the crude mixtures indicated formation of doubly fused products. **2d-Cu**: HRMS: 1143.4449 ($MH^+$), calcd. 1143.4500 for $C_{80}H_{65}N_4Cu$. **2d-Mg**: HRMS: 1104.4953 ($M^+$), calcd. 1104.4976 for $C_{80}H_{64}N_4Mg$. **2d-Pd**: MADLI TOF: 1186,10 ($M^+$), calcd. 1186.42 for $C_{80}H_{64}N_4Pd$. **2d-Pt**: HRMS: 1276.4859 ($MH^+$), calcd. 1276.4852 for $C_{80}H_{65}N_4Pt$.

*Device Fabrication and Characterization.* CuPc (Aldrich; 97%), $C_{60}$ (MER; 99+%), and bathocuproine (Aldrich; 96%) were obtained from commercial sources and purified via thermal gradient sublimation (~0.2 $\mu$Torr). Aluminum (Alfa Aesar; 99.999%) was used as received. Glass substrates commercially coated with ITO (thickness: 1500 ± 100 Å, sheet resistance: 20 ± 5 Ω/cm$^2$, transmission: 84% at 550 nm) were purchased from Thin Film Devices Inc.

*Film Growth and Characterization.* Device substrates were solvent cleansed and placed in an ozone atmosphere for 10 min immediately before loading into the high vacuum (~3 $\mu$Torr) deposition chamber. Layer thicknesses and deposition rates were monitored by a quartz crystal microbalance calibrated using monochromatic or spectroscopic ellipsometry. Materials were sequentially grown by vacuum thermal evaporation at the following rates: $C_{60}$ (2−4 Å/s), BCP (2 Å/s), Al (5 Å/s), porphyrin **2d** (1−2 Å/s). The base pressure during deposition of porphyrin **2d** was 1−5 × $10^{-5}$ Torr due to partial decomposition of organic material. Condensed phase optical measurements were performed on solvent-cleansed glass, quartz, or polished silicon substrates using an Agilent 8453 spectrophotometer and a Photon Technology International fluorimeter.

*Device Characterization.* Current−voltage measurements were performed in ambient conditions using a SourceMeter in the dark and under corrected 1000 Wm$^{2-}$ white light illumination from a 300 W xenon arc lamp. Spectral mismatch correction was performed as described in the literature[39,46] using a silicon photodiode, calibrated at the National Renewable Energy Laboratory (NREL), and frequency modulated illumination (250 Hz) from a Xe source coupled to a 1/4 M monochromator in conjunction with an Lock-In amplifier. This monochromatic system was also used to collect all external quantum efficiency data.

## ■ ASSOCIATED CONTENT

### Ⓢ Supporting Information

$^1$H and $^{13}$C NMR and mass spectra for compounds **1**−**4**, **2-H**, **2-Mg**, **2-Cu**, **2-Pb**, **2-Pt**, **2d**, **3d**, **5**; cyclic voltammetry traces for **2**, **2m** and **2d**, details of molecular modeling studies, including optimized geometries performed on model compounds **1d′**−**4d′** and $\pi$-extended analogs. This material is available free of charge via the Internet at http://pubs.acs.org.

## ■ AUTHOR INFORMATION

### Corresponding Author

*met@usc.edu

## ■ ACKNOWLEDGMENTS

We acknowledge Drs. Matthew Whited and Peter Djurovich for helpful discussion. The Department of Energy, Office of Basic Energy Sciences as part of Energy Frontier Research Center program, the Center for Energy Nanoscience (DE-SC0001013) are acknowledged for support of the OPV studies of compound **2d** (C.W.S. and J.D.Z.). We also acknowledge the NSF SOLAR program (Award ID 0934098, S.R.F and Q.Z.), Universal Display Corporation, Global Photonic Energy Corporation and the Center for Advanced Molecular Photovoltaics (CAMP) (KUS-C1-015-21) of the King Abdullah University of Science and Technology (KAUST) for financial support of the other science presented here.

## ■ REFERENCES

(1) Kadish, K.; Smith, K.; Guilard, R. *The Handbook of Porphyrin Science*; World Scientific: Hackensack, NJ, 2010.

(2) For reviews, see: (a) Peumans, P.; Yakimov, A.; Forrest, S. R. *J. Appl. Phys.* **2003**, *93*, 3693. (b) Imahori, H.; Umeyama, T.; Ito, S. *Acc. Chem. Res.* **2009**, *42*, 1809. (c) Campbell, W. M.; Burrell, A. K.; Officer, D. L.; Jolley, K. W. *Coord. Chem. Rev.* **2004**, *248*, 1363. (d) Walter, M. G.; Rudine, A. B.; Wamser, C. C. *J. Porphyrins Phthalocyanines* **2010**, *14*, 759. (e) Radivojevic, I.; Varotto, A.; Farley, C.;

Drain, C. M. *Energy Environ. Sci.* **2010**, *3*, 1897. (f) Martínez-Díaz, M. V.; de la Torre, G.; Torres, T. *Chem. Commun.* **2010**, *46*, 7090.

(3) Recent selected examples: (a) Perez, M. D.; Borek, C.; Forrest, S. R.; Thompson, M. E. *J. Am. Chem. Soc.* **2009**, *131*, 9281. (b) Perez, M. D.; Borek, C.; Djurovich, P. I.; Mayo, E. I.; Lunt, R. R.; Forrest, S. R.; Thompson, M. E. *Adv. Mater.* **2009**, *21*, 1517. (c) Kinoshita, Y.; Takenaka, R.; Murata, H. *Appl. Phys. Lett.* **2008**, *92*, 243309. (d) Shao, Y.; Yang, Y. *Adv. Mater.* **2005**, *17*, 2841. (e) Kira, A.; Matsubara, Y.; Iijima, H.; Umeyama, T.; Matano, Y.; Ito, S.; Niemi, M.; Tkachenko, N. V.; Lemmetyinen, H.; Imahori, H. *J. Phys. Chem. C.* **2010**, *114*, 11293. (f) Bessho, T.; Zakeeruddin, S. M.; Yeh, C.-Y.; Diau, W.-G.; Grätzel, M. *Angew. Chem., Int. Ed.* **2010**, *49*, 6646. (g) Mai, C.-L.; Huang, W.-K.; Lu, H.-P.; Lee, C.-W; Chiu, C.-L.; Liang, Y.-R.; Diau, E. W.-G.; Yeh, C.-Y. *Chem. Commun.* **2010**, *46*, 809.

(4) (a) Zimmerman, J. D.; Diev, V. V.; Hanson, K.; Lunt, R. R.; Yu, E. K.; Thompson, M. E.; Forrest, S. R. *Adv. Mater.* **2010**, *22*, 2780. (b) Zimmerman, J. D.; Yu, E. K.; Diev, V. V.; Hanson, K.; Thompson, M. E.; Forrest, S. R. *Org. Electron.* **2011**, *12*, 869.

(5) (a) Baldo, M. A.; O'Brien, D. F.; You, Y.; Shoustikov, A.; Sibley, S.; Thompson, M. E.; Forrest, S. R. *Nature* **1998**, *395*, 151. (b) Borek, C.; Hanson, K.; Djurovich, P. I.; Thompson, M. E.; Aznavour, K.; Bau, R.; Sun, Y.; Forrest, S. R.; Brooks, J.; Michalski, L.; Brown, J. *Angew. Chem., Int. Ed.* **2007**, *46*, 1109. (c) Sommer, J. R.; Farley, R. T.; Graham, K. R.; Yang, Y.; Reynolds, J. R.; Xue, J.; Schanze, K. S. *ACS Appl. Mater. Interfaces* **2009**, *1*, 274. (d) Fenwick, O.; Sprafke, J. K.; Binas, J.; Kondratuk, D. V.; Di Stasio, F.; Anderson, H. L.; Cacialli, F. *Nano Lett.* **2011**, *11*, 2451.

(6) (a) Murphy, A. R.; Fréchet, J. M. J. *Chem. Rev.* **2007**, *107*, 1066. (b) Che, C.-M.; Xiang, H.-F.; Chui, S. S.-Y.; Xu, Z.-X.; Roy, V. A. L.; Yan, J. J.; Fu, W.-F.; Lai, P. T.; Williams, I. D. *Chem. Asian J.* **2008**, *3*, 1092. (c) Aramaki, S.; Sakai, Y.; Ono, N. *Appl. Phys. Lett.* **2004**, *84*, 2085. (d) Noh, Y.-Y.; Kim, J.-J.; Yoshida, Y.; Yase, K. *Adv. Mater.* **2003**, *15*, 699. (e) Shea, P. B.; Kanicki, J.; Ono, N. *J. Appl. Phys.* **2005**, *98*, 014503. (f) Checcoli, P.; Conte, G.; Salvatori, S.; Paolesse, R.; Bolognesi, A.; Berliocchi, A.; Brunetti, F.; D'Amico, A.; Di Carlo, A.; Lugli, P. *Synth. Met.* **2003**, *138*, 261.

(7) (a) Forrest, S. R. *Nature* **2004**, *428*, 911. (b) Granström, M.; Petritsch, K.; Arias, A. C.; Lux, A.; Andersson, M. R.; Friend, R. H. *Nature* **1998**, *395*, 257. (c) Yu, G.; Gao, J.; Hummelen, J. C.; Wudl, F.; Heeger, A. J. *Science* **1995**, *270*, 1789.

(8) (a) Pandey, R. K.; Bellinger, D. A.; Smith, K. D.; Dougherty, T. J. *Photochem. Photobiol.* **1991**, *53*, 65. (b) Bonnett, R. *Chem. Soc. Rev.* **1995**, *24*, 19. (c) Sternberg, E. D.; Dolphin, D.; Brückner, C. *Tetrahedron* **1998**, *54*, 4151. (d) Dougherty, T. J.; Gomer, C. J.; Henderson, B. W.; Jori, G.; Kessel, D.; Korbelik, M.; Moan, J.; Peng, Q. *J. Natl. Cancer Inst.* **1998**, *90*, 889.

(9) (a) Senge, M. O.; Fazekas, M.; Notaras, E. G. A.; Blau, W. J.; Zawadzka, M.; Locos, O. B.; Ni Mhuircheartaigh, E. M. *Adv. Mater.* **2007**, *19*, 2737. (b) Pawlicki, M.; Collins, H. A.; Denning, R. G.; Anderson, H. L. *Angew. Chem., Int. Ed.* **2009**, *48*, 3244 and references therein.

(10) (a) Lash, T. D. *J. Porphyrins Phthalocyanines* **2001**, *5*, 267. (b) Lash, T. D.; Chandrasekar, P. *J. Am. Chem. Soc.* **1996**, *118*, 8767.

(11) (a) Anderson, H. L. *Inorg. Chem.* **1994**, *33*, 972. (b) Anderson, H. L.; Martin, S. J.; Bradley, D. D. C. *Angew. Chem., Int. Ed. Engl.* **1994**, *33*, 655. (c) Lin, V. S. Y.; DiMagno, S. G.; Therien, M. J. *Science*, *264*, 1105. (d) Anderson, H. L. *Chem. Commun.* **1999**, 2323. (e) Screen, T. E. O.; Blake, I. M.; Rees, L. H.; Clegg, W.; Borwick, S. J.; Anderson, H. L. *J. Chem. Soc., Perkin. Trans. 1* **2002**, 320. (f) Duncan, T. V.; Susumu, K.; Sinks, L. E.; Therien, M. J. *J. Am. Chem. Soc.* **2006**, *128*, 9000. (g) Arnold, D. P.; Nitschinsk, L. J. *Tetrahedron* **1992**, *48*, 8781. (h) Anderson, H. L; Sanders, J. K. M. *J. Chem. Soc., Chem. Commun.* **1989**, 1714.

(12) (a) Tsuda, A.; Furuta, H.; Osuka, A. *Angew. Chem., Int. Ed.* **2000**, *39*, 2549. (b) Tsuda, A.; Osuka, A. *Science* **2001**, *293*, 79. (c) Tsuda, A.; Furuta, H.; Osuka, A. *J. Am. Chem. Soc.* **2001**, *123*, 10304. (d) Cho, H. S.; Jeong, D. H.; Cho, S.; Kim, D.; Matsuzaki, Y.; Tanaka, K.; Tsuda, A.; Osuka, A. *J. Am. Chem. Soc.* **2002**, *124*, 14642. (e) Ikeda, T.; Aratani, N.; Osuka, A. *Chem. Asian J.* **2009**, *4*, 1248.

(13) (a) Kim, P.; Ikeda, T.; Lim, J. M.; Park, J.; Lim, M.; Aratani, N.; Osuka, A.; Kim, D. *Chem. Commun.* **2011**, *47*, 4433. (b) Frampton, M. J.; Accorsi, G.; Armaroli, N.; Rogers, J. E.; Fleitz, P. A.; McEwan, K. J.; Anderson, H. L. *Org. Biomol. Chem.* **2007**, *5*, 1056.

(14) (a) Watson, M. D.; Fechtenkötter, A.; Müllen, K. *Chem. Rev.* **2001**, *101*, 1267. (b) Yamamoto, Y.; Fukushima, T.; Suna, Y.; Ishii, N.; Saeki, A.; Seki, S.; Tagawa, S.; Taniguchi, M.; Kawai, T.; Aida, T. *Science* **2006**, *314*, 1761. (c) Wu, J.; Pisula, W.; Müllen, K. *Chem. Rev.* **2007**, *107*, 718. (d) Zhi, L.; Müllen, K. *J. Mater. Chem.* **2008**, *18*, 1472. (e) Li, C.; Liu, M.; Pschirer, N. G.; Baumgarten, M.; Müllen, K. *Chem. Rev.* **2010**, *110*, 6817. (f) Dössel, L.; Gherghel, L.; Feng, X. L.; Müllen, K. *Angew. Chem., Int. Ed.* **2011**, *50*, 2540. (g) Pisula, W.; Feng, X.; Müllen, K. *Chem. Mater.* **2011**, *23*, 554.

(15) (a) Yamane, O.; Sugiura, K.-I.; Miyasaka, H.; Nakamura, K.; Fujimoto, T.; Nakamura, K.; Kaneda, T.; Sakata, Y.; Yamashita, M. *Chem. Lett.* **2004**, *33*, 40. (b) Kurotobi, K.; Kim, K. S.; Noh, S. B.; Kim, D.; Osuka, A. *Angew. Chem., Int. Ed.* **2006**, *45*, 3944. (c) Tanaka, M.; Hayashi, S.; Eu, S.; Umeyama, T.; Matano, Y.; Imahori, H. *Chem. Commun.* **2007**, 2069. (d) Davis, N. K. S.; Pawlicki, M.; Anderson, H. L. *Org. Lett.* **2008**, *10*, 3945. (e) Davis, N. K. S.; Thompson, A. L; Anderson, H. L. *Org. Lett.* **2010**, *12*, 2124. (f) Jiao, C.; Huang, K.-W.; Guan, Z.; Xu, Q.-H.; Wu, J. *Org. Lett.* **2010**, *12*, 4046. (g) Davis, N. K. S.; Thompson, A. L.; Anderson, H. L. *J. Am. Chem. Soc.* **2011**, *133*, 30. (h) Jiao, C.; Huang, K.-W.; Chi, C.; Wu, J. *J. Org. Chem.* **2011**, *76*, 661. (i) Cammidge, A. N.; Scaife, P. J.; Berber, G.; Hughes, D. L. *Org. Lett.* **2005**, *7*, 3413. (j) Jiao, C.; Zu, N.; Huang, K.-W.; Wang, P.; Wu, J. *Org. Lett.* **2011**, *13*, 3652. (k) Lewtak, J. P.; Gryko, D.; Bao, D.; Sebai, E.; Vakuliuk, O.; Ścigaj, M.; Gryko, D. T. *Org. Biomol. Chem.* **2011**, *9*, 8178.

(16) For other representative examples of porphyrins with extended conjugation, see: (a) Lash, T. D.; Werner, T. M.; Thompson, M. L.; Manley, J. M. *J. Org. Chem.* **2001**, *66*, 3152. (b) Richeter, S.; Jeandon, C.; Kyritsakas, N.; Ruppert, R.; Callot, H. J. *J. Org. Chem.* **2003**, *68*, 9200. (c) Gill, H. S.; Harmjanz, M.; Santamaria, J.; Finger, I.; Scott, M. J. *Angew. Chem., Int. Ed.* **2004**, *43*, 485. (d) Tokuji, S.; Takahashi, Y.; Shinmori, H.; Shinokubo, H.; Osuka, A. *Chem. Commun.* **2009**, 1028. Recent examples: (e) Akhigbe, J.; Zeller, M.; Brückner, C. *Org. Lett.* **2011**, *13*, 1322. (f) Jiao, C.; Zhu, L.; Wu, J. *Chem.—Eur. J.* **2011**, *17*, 6610. (g) Jiang, L.; Engle, J. T.; Sirk, L.; Hartley, C. S.; Ziegler, C. J.; Wang, H. *Org. Lett.* **2011**, *13*, 3020. (h) Jeandon, C.; Ruppert, R. *Eur. J. Org. Chem.* **2011**, 4098. (i) Boerner, L. J. K.; Nath, M.; Pink, M.; Zaleski, J. M. *Chem.—Eur. J.* **2011**, *17*, 9311. (j) Xu, H.-J.; Mack, J.; Descalzo, A. B.; Shen, Z.; Kobayashi, N.; You, X.-Z.; Rurack, K. *Chem.—Eur. J.* **2011**, *17*, 8965.

(17) Diev, V. V.; Hanson, K.; Zimmerman, J. D.; Forrest, S. R.; Thompson, M. E. *Angew. Chem., Int. Ed.* **2010**, *49*, 5523.

(18) (a) Kim, D.; Kirmaier, C.; Holten, D. *Chem. Phys.* **1983**, *75*, 305. (b) Rodriguez, J.; Holten, D. *J. Chem. Phys.* **1989**, *91*, 3525. (c) Eom, H. S.; Jeoung, S. C.; Kim, D.; Ha, J.-H.; Kim, Y.-R. *J. Phys. Chem. A* **1997**, *101*, 3661. (d) Yoon, M.-C.; Noh, S. B.; Tsuda, A.; Nakamura, Y.; Osuka, A.; Kim, D. *J. Am. Chem. Soc.* **2007**, *129*, 10080. (e) Chen, L. X.; Zhang, X.; Wasinger, E. C.; Attenkofer, K.; Jennings, G.; Muresan, A. Z.; Lindsey, J. S. *J. Am. Chem. Soc.* **2007**, *129*, 9616. (f) Nobukuni, H.; Shimazaki, Y.; Udo, H.; Naruta, Y.; Ohkubo, K.; Kojima, T.; Fukuzumi, S.; Seki, S.; Sakai, H.; Hasobe, T.; Tani, F. *Chem.—Eur. J.* **2010**, *16*, 11611.

(19) (a) Katsu, T.; Tamagake, K.; Fujita, Y. *Chem. Lett.* **1980**, 289. (b) Nevin, W. A.; Chamberlain, G. A. *J. Chem. Soc., Faraday Trans. 2* **1989**, *85*, 1747. (c) Lin, C.-Y.; Lo, C.-F.; Hsieh, M.-H.; Hsu, S.-J.; Lu, H.-P.; Diau, E. W.-G. *J. Chin. Chem. Soc.* **2010**, *57*, 1136.

(20) (a) Desiraju, G. R.; Gavezzotti, A. *J. Chem. Soc., Chem. Commun.* **1989**, 621. (b) Desiraju, G. R.; Gavezzotti, A. *Acta Crystallogr., Sect. B* **1989**, *45*, 473.

(21) (a) Coropceanu, V.; Cornil, J.; da Silva Filho, D. A.; Olivier, Y.; Silbey, R.; Brédas, J.-L. *Chem. Rev.* **2007**, *107*, 926. (b) Hains, A. W.; Liang, Z.; Woodhouse, M. A.; Gregg, B. A. *Chem. Rev.* **2010**, *110*, 6689. (c) Liu, C.-y.; Bard, A. J. *Nature* **2002**, *418*, 162. (d) Brédas, J. L.; Calbert, J. P.; da Silva Filho, D. A.; Cornil, J. *Proc. Natl. Acad. Sci. U.S.A.* **2002**, *99*, 5804.

(22) (a) Brédas, J.-L.; Beljonne, D.; Coropceanu, V.; Cornil, J. *Chem. Rev.* **2004**, *104*, 4971. (b) Würthner, F.; Kaiser, T. E.; Saha-Möller, C. R. *Angew. Chem., Int. Ed.* **2011**, *50*, 3376. (c) Johns, J. E.; Muller, E. A.; Frechet, J. M. J.; Harris, C. B. *J. Am. Chem. Soc.* **2010**, *132*, 15720.
(23) Kazmaier, P. M.; Hoffmann, R. *J. Am. Chem. Soc.* **1994**, *116*, 9684.
(24) (a) Cheng, F.; Zhang, S.; Adronov, A.; Echegoyen, L.; Diederich, F. *Chem.—Eur. J.* **2006**, *12*, 6062. (b) DiMagno, S. G.; Lin, V. S.-Y.; Therien, M. J. *J. Am. Chem. Soc.* **1993**, *115*, 2513. (c) DiMagno, S. G.; Lin, V. S.-Y.; Therien, M. J. *J. Org. Chem.* **1993**, *58*, 5983. (d) Shi, B.; Boyle, R. W. *J. Chem. Soc., Perkin Trans. 1* **2002**, 1397. (e) Ren, T. *Chem. Rev.* **2008**, *108*, 4185.
(25) (a) Lindsey, J. S.; Schreiman, I. C.; Hsu, H. C.; Kearney, P. C.; Marguerettaz, A. M. *J. Org. Chem.* **1987**, *52*, 827. (b) Lee, C.-H.; Lindsey, J. S. *Tetrahedron* **1994**, *50*, 11427. (c) Laha, J. K.; Dhanalekshmi, S.; Taniguchi, M.; Ambroise, A.; Lindsey, J. S. *Org. Process Res. Dev.* **2003**, *7*, 799. (d) Lindsey, J. S. *Acc. Chem. Res.* **2010**, *43*, 300.
(26) Harriman, A.; Davila, J. *Tetrahedron* **1989**, *45*, 4737.
(27) (a) Clar, E.; Sanigok, U.; Zander, M. *Tetrahedron* **1968**, *24*, 2817. (b) Schulman, J. M.; Disch, R. L. *J. Phys. Chem. A* **1997**, *101*, 9176. (c) Gomes, J. A. N. F.; Mallion, R. B. *Chem. Rev.* **2001**, *101*, 1349.
(28) Bröring, M. *Angew. Chem., Int. Ed.* **2011**, *50*, 2436.
(29) (a) Scholl, R.; Seer, C.; Weitzenböock, R. *Ber. Dtsch. Chem. Ges.* **1910**, *43*, 2202. (b) Scholl, R.; Seer, C. *Liebigs Ann. Chem.* **1912**, *394*, 111. (c) Scholl, R.; Seer, C. *Ber. Dtsch. Chem. Ges.* **1922**, *55*, 330. (d) Kovacic, P.; Jones, M. B. *Chem. Rev.* **1987**, *87*, 357. (e) King, B. T.; Kroulík, J.; Robertson, C. R.; Rempala, P.; Hilton, C. L.; Korinek, J. D.; Gortari, L. M. *J. Org. Chem.* **2007**, *72*, 2279. (f) Sarhan, A. A. O.; Bolm, C. *Chem. Soc. Rev.* **2009**, *38*, 2730.
(30) Davis, A. P.; Fry, A. J. *J. Phys. Chem. A* **2010**, *114*, 12299 and references therein.
(31) (a) Tsefrikas, V. M.; Scott, L. T. *Chem. Rev.* **2006**, *106*, 4868. (b) McNab, H. *Aldrchim. Acta* **2004**, *37*, 19. (c) Brown, R. F. C. *Eur. J. Org. Chem.* **1999**, 3211.
(32) (a) Yamada, H.; Okujima, T.; Ono, N. *Chem. Commun.* **2008**, 2957. (b) Matsuo, Y.; Sato, Y.; Niinomi, T.; Soga, I.; Tanaka, H.; Nakamura, E. *J. Am. Chem. Soc.* **2009**, *131*, 16048. (c) Cai, J.; Ruffieux, P.; Jaafar, R.; Bieri, M.; Braun, T.; Blankenburg, S.; Muoth, M.; Seitsonen, A. P.; Saleh, M.; Feng, X.; Müllen, K.; Fasel, R. *Nature* **2010**, *466*, 470.
(33) (a) Ito, S.; Murashima, T.; Uno, H.; Ono, N. *Chem. Commun.* **1998**, 1661. (b) Aihara, H.; Jaquinod, L.; Nurco, D. J.; Smith, K. M. *Angew. Chem., Int. Ed.* **2001**, *40*, 3439.
(34) (a) Wasserfallen, D.; Kastler, M.; Pisula, W.; Hofer, W. A.; Fogel, Y.; Wang, Z.; Müllen, K. *J. Am. Chem. Soc.* **2006**, *128*, 1334. (b) Pascal, R. A. Jr. *Chem. Rev.* **2006**, *106*, 4809. (c) Finikova, O. S.; Cheprakov, A. V.; Carroll, P. J.; Vinogradov, S. A. *J. Org. Chem.* **2003**, *68*, 7517.
(35) (a) D'Andrade, B. W.; Datta, S.; Forrest, S. R.; Djurovich, P. I.; Polikarpov, E.; Thompson, M. E. *Org. Electron.* **2005**, *6*, 11. (b) Djurovich, P. I.; Mayo, E. I.; Forrest, S. R.; Thompson, M. E. *Org. Electron.* **2009**, *10*, 515.
(36) (a) Hunter, C. A.; Sanders, J. K. M. *J. Am. Chem. Soc.* **1990**, *112*, 5525. (b) Hunter, C. A.; Lawson, K. R.; Perkins, J.; Urch, C. J. *J. Chem. Soc., Perkin Trans. 2* **2001**, 651.
(37) (a) Englman, R.; Jortner, J. *Mol. Phys.* **1970**, *18*, 145. (b) Berezin, M. Y.; Achilefu, S. *Chem. Rev.* **2010**, *110*, 2641.
(38) Gadisa, A.; Svensson, M.; Andersson, M. R.; Inganas, O. *Appl. Phys. Lett.* **2004**, *84*, 1609.
(39) Shrotriya, V.; Li, G.; Yao, Y.; Moriarty, T.; Emery, K.; Yang, Y. *Adv. Funct. Mater.* **2006**, *16*, 2016.
(40) (a) Shediac, R.; Gray, M. H. B.; Uyeda, H. T.; Johnson, R. C.; Hupp, J. T.; Angiolillo, P. J.; Therien, M. J. *J. Am. Chem. Soc.* **2000**, *122*, 7017. (b) Plater, M. J.; Aiken, S.; Bourhill, G. *Tetrahedron* **2002**, *58*, 2405.
(41) Newman, M. S.; Lee, L. F. *J. Org. Chem.* **1972**, *37*, 4468.
(42) Murata, M.; Oyama, T.; Watanabe, S.; Masuda, Y. *J. Org. Chem.* **2000**, *65*, 164.
(43) Beinhoff, M.; Weigel, W.; Jurczok, M.; Rettig, W.; Modrakowski, C.; Brüdgam, I.; Hartl, H.; Schlüter, A. D. *Eur. J. Org. Chem.* **2001**, 3819.
(44) Morandi, S.; Caselli, E.; Forni, A.; Bucciarelli, M.; Torre, G.; Prati, F. *Tetrahedron: Asymmetry* **2005**, *16*, 2918.
(45) Avlasevich, Y.; Müllen, K. *J. Org. Chem.* **2007**, *72*, 10243.
(46) (a) Emery, K. In *Handbook of Photovoltaic Science and Engineering*; Luque., A. H. S., Ed.; Wiley & Sons: Chichester, U.K., 2003. (b) Matson, R. J.; Emery, K. A.; Bird, R. E. *Sol. Cells* **1984**, *11*, 105.